

R-01-53

Rock mechanical conditions at the Äspö HRL

A study of the correlation between geology, tunnel maintenance and tunnel shape

Christer Andersson
Svensk Kärnbränslehantering AB

Jörgen Söderhäll
SWECO

December 2001

Svensk Kärnbränslehantering AB

Swedish Nuclear Fuel
and Waste Management Co
Box 5864
SE-102 40 Stockholm Sweden
Tel 08-459 84 00
+46 8 459 84 00
Fax 08-661 57 19
+46 8 661 57 19



Rock mechanical conditions at the Äspö HRL

A study of the correlation between geology, tunnel maintenance and tunnel shape

Christer Andersson
Svensk Kärnbränslehantering AB

Jörgen Söderhäll
SWECO

December 2001

Keywords: Numerical modelling, Scaling, Bolting, Shotcrete, Water inflow, Geological model, Fracture zones, Tunnel layout, In situ stress.

Summary

Maintenance records including scaling, shotcreting and bolting have been kept since the excavation start of Äspö HRL 1990 together with records of groundwater flow and all other activities taking place in the tunnels. When the facility was constructed one objective was to limit the rock support as much as possible. The reason for this was that it should be possible to go back and easily study the exposed rock surface. Support during the operational phase has only been carried out where and when necessary. This type of maintenance and its location is documented in the digital database each time.

The maintenance records have been compiled and areas requiring more maintenance than average noted. An interview has also been held with one of the miners conducting scaling and bolting in the tunnel. His experiences together with the study of the database maintenance records led to the selection of certain areas in the tunnel to be studied by numerical modelling. The probable reason for the need of additional maintenance in all areas, not only these numerically modelled, has been investigated.

Almost all maintenance in the main tunnel both during construction and the operational phase has been located in the widened curves of the access tunnel. The maintenance is also located in areas containing veins or intrusions of Småland granite or Fine-grained granite. These areas are often located in fracture zones of different sizes or show an increasing fracture frequency. The areas numerically modelled indicate stress concentrations or unloaded stress conditions. The stress concentrations are created by the geometry of the niches and side-tunnels in relation to the in situ stress field.

The angle between the tunnel and the major principal stress has an impact on the need for maintenance. The areas with the largest angles towards the principal stress direction need more maintenance than the areas almost parallel to the major principal stress direction.

The maintenance work in the horseshoe shaped tunnel TASF at the 450 m level has been compared to the maintenance work in the adjacent TBM tunnel. No maintenance has been performed in the TBM tunnel but TASF have been scaled and bolted several times and was finally shotcreted. The TASF tunnel has some larger areas with Småland granite and fine-grained granite. The modelling does not indicate problems due to stress concentrations. It is therefore probable that the granites are rather fractured and therefore needs more scaling.

The water flow in the Äspö HRL is continually monitored. During the first five years of operation the water flow has had an average decrease of approximately 4% per year. The water flow in two other facilities owned by SKB, SFR and CLAB has been monitored for the last 12 years. These two facilities also show a decrease of the water flow of approximately 4% per year.

Sammanfattning

Sedan byggnationen av Äspölaboratoriet startade har uppgifter om aktiviteter som ägt rum i tunnlarna samt bland annat data om inläckaget registrerats och arkiverats. För det bergunderhåll som utförts har uppgifter om skrotning, bultning och användande av sprutbetong arkiverats. En målsättning som sattes upp vid byggandet av anläggningen var att endast utföra förstärkningsåtgärder vid de delar av tunnelsystemet som verkligen behövde det av säkerhetsskäl. Målsättningen sattes upp eftersom det i efterhand skulle vara enkelt att studera bergytan i en så stor del av anläggningen som möjligt. Ytterligare förstärkningsåtgärder har under Äspölaboratoriets driftsfas endast utförts då det bedömts som nödvändigt av säkerhetsskäl. Typen av underhåll och dess läge i tunneln tillsammans med mängden har sedan arkiverats i den digitala databasen vid varje enskilt tillfälle.

En sammanställning har gjorts av bergunderhållsdokumenterna och de områden som har behövt mer underhåll än genomsnittet i tunnelsystemet har identifierats och förklaringar till detta sökts. En intervju med en av de yrkesarbetare som genomfört skrotning och bultning har även genomförts. De personliga erfarenheterna tillsammans med materialet från databasen har sedan använts för att välja ut ett antal av de områden som underhållits mer än genomsnittet. Spänningsfältet runt de valda områdena har sedan beräknats genom numerisk modellering.

Huvuddelen av bergunderhållet i tunnlarna från byggtiden till dagsläget är koncentrerat till kurvorna där tunnelarean ökats. Även områden som innehåller gångar av Smålandsgranit och finkornig granit har krävt relativt mer underhåll. Detta förklaras med att dessa bergarter ofta är belägna i deformationszoner och överhuvudtaget är mer uppspruckna än Äspödioriten. De områden som modellerats numeriskt påvisar att de extra underhållna områdena kan associeras till volymer som antingen är avlastade eller utsatta för spänningskoncentrationer. Spänningskoncentrationerna och avlastningarna beror på de modellerade områdenas faktiska geometri i förhållande till huvudspänningarna. De observationer som gjorts i tunnelsystemet stämmer generellt sett bra med de resultat som framgår av den numeriska modelleringen.

Vinkeln mellan de olika tunnlarna och riktningen på den största huvudspänningen påverkar behovet av bergunderhåll. De tunneldelar som har den största vinkeln mot huvudspänningen kräver en större underhållsinsats än de tunneldelar som ligger mer eller mindre parallellt med huvudspänningsriktningen.

Behovet av bergunderhåll i den hästskoformade sprängda tunneln TASF på 450 m djup har jämförts med den omedelbart intilliggande TBM tunneln. TBM tunneln har varit underhållsfri medan TASF har fått skrotas och bultas vid ett flertal tillfällen innan slutligen tunnelväggarna täcktes av sprutbetong. TASF innehåller områden med stora inslag av Smålandsgranit och finkornig granit. Den numeriska modelleringen kan inte förklara den stora skillnaden i underhåll. Det är därför troligt att graniterna är mer uppspruckna än Äspödioriten i TBM tunneln och därför krävt mer underhåll.

Vatteninflödet till Äspölaboratoriet har mätts sedan driftsfasen startade. Under de fem år som mätningarna hittills pågått har det totala vatteninflödet minskat med i genomsnitt 4 % per år. Vatteninflödet i två andra berganläggningar ägda av SKB, SFR och CLAB har mätts under de senaste tolv åren. Även dessa anläggningar påvisar ett inflöde som sjunker med cirka 4 % per år.

Contents

	Page
1 Introduction	7
2 Site description	9
2.1 Geology	9
2.1.1 Rock types	10
2.1.2 Tectonics	12
2.2 State of stress	15
2.3 Site layout	20
2.3.1 Tunnel dimensions	20
2.4 Construction	21
2.4.1 Rock support and grouting	21
3 Maintenance	23
3.1 Interview	23
3.2 Maintenance records	24
3.2.1 Rock mass quality	24
3.2.2 Scaling, bolting and shotcreting	25
3.2.3 Compilation of scaling, bolting and shotcreting records	26
3.2.4 Compilation of water inflow records	28
3.3 Maintenance in TBM and D&B tunnels	30
4 Numerical modelling	33
4.1 Strategy	33
4.2 Areas with significant maintenance records	35
4.3 Modelling results	37
4.3.1 NASA 3009A	37
4.3.2 T ASD and T ASO	40
4.3.3 NASA 3419B	43
4.3.4 T ASJ and its crossing with T ASA and T ASI	47
4.3.5 NASJ 0015B	49
4.3.6 Comparison TBM and D&B	52
5 Discussion	55
5.1 Maintenance	55
5.2 Water inflow	56
5.3 Numerical modelling	56
6 Conclusions	61
References	63

1 Introduction

In 1986 SKB decided to construct an underground hard rock laboratory (HRL) in order to provide an opportunity for research, development and method demonstration in a realistic and undisturbed underground rock environment down to the depth planned for a future deep repository. In the autumn of 1986, SKB initiated fieldworks for the siting of an underground laboratory in the Simpevarp area, in the municipality of Oskarshamn. At the end of 1988, SKB decided to site the laboratory on southern Äspö about 2 km north of the Oskarshamn nuclear power station, see Figure 2-1. Construction of the Äspö HRL started on October 1st, 1990 after approval had been obtained from the authorities concerned. The excavation work was completed in February 1995.

The Äspö HRL has been designed to meet the needs for the research-, development- and demonstration-projects that are planned for the operating phase. The underground part of the laboratory consists of a tunnel from the Simpevarp peninsula to the southern part of Äspö where the tunnel continues in a spiral down to a depth of 450 m. The total length of the tunnel is 3600 m out of which the last 400 m have been excavated with the use of a tunnel-boring machine (TBM) with a diameter of 5 m. The first part of the tunnel has been excavated by conventional drill and blast techniques. The tunnels are connected with the ground surface through a hoist shaft and two ventilation shafts.

During the construction phase of the laboratory 1990–1995 comprehensive investigations and experiments were performed in conjunction with the construction work. Excavating records as well as support records were archived.

The operating phase of the laboratory began in 1995. Comprehensive documentation regarding all performed experiments, maintenance measures taken and other related activities have been done. The activity records from the construction phase as well as from the operating phase have been stored in both an ordinary archive and digitally in the Site Characterisation Database (SICADA).

This report focuses on the stability of the existing tunnels and niches at Äspö HRL and one of the objectives was to correlate maintenance with rock mechanics factors, e.g. stress concentrations, tensile stress zones, fracture frequency, tunnel orientation relative to in situ stress orientation. Such information would benefit the design of the repository. The extensive records can be used to locate parts of the tunnels that have required more maintenance than average.

To identify areas that need more maintenance than average the maintenance records have been studied and an interview held with one of the miners. The approach has given a reasonably complete picture of the maintenance situation in the tunnel system. Some of the identified areas where the need for additional maintenance couldn't be explained by adverse geology have been numerically modelled.

2 Site description

The Äspö HRL is located in the area of Simpevarp in the northeastern part of the municipality of Oskarshamn. The geographical location of the Äspö HRL is given in Figure 2-1.



Figure 2-1. Geographical location of Äspö HRL. The red line is the planar view of the tunnel layout.

2.1 Geology

Information about the geology at the Äspö HRL is derived from Rhén et al /1997/. Igneous rocks belonging to the 1700–1800 million year-old Småland granite suite dominate Äspö. There are mafic enclaves and dikes probably formed in a magma-mingling and magma-mixing process resulting in a very inhomogeneous rock mass mineralogical composition. The major principal stress component during the forming of the rock mass was trending NNW-SSE. The stress direction is indicated by the most dominant structural element in the Äspö granitoids which is a steep penetrating foliation trending NE-ESE. The foliation is ductile and was formed when the rock mass was deep down and relatively hot. All rock masses at Äspö are intruded by fine-grained granite of two or three generations.

The tectonic picture is dominated by two almost orthogonal systems of major structures, one trending N-S and E-W and the second trending NW and NE. Their extension is larger than 10 km.

The first brittle jointing and faulting probably occurred 1400 million years ago when anorogenic granites formed massifs in the older bedrock. One of these intrusions was located in Göttemar located approximately 2 km north of Äspö. Reactivation of faults and older ductile zones occurred several times as the rock mass was uplifted and unceilinged about 1000 million years ago. The net slip for the large faults was approximately 30 cm and 1 cm for the smaller faults.

Dikes in the rock mass filled with Cambrian sandstone indicate that the stress field was rotated about 90 degrees sometime between 1000 and 500 million years ago. The directions of the principal stresses are now approximately the same as 1800 million years ago, see section 2.2.

2.1.1 Rock types

The four most common rock types in the Äspö HRL are the Äspö diorite followed by Småland granite, Greenstone and Fine-grained granite. Figure 2-2 shows an overview of the mapping and the approximate distribution of the different rock types at different levels.

The Äspö diorite is by far the most common rock type and is grey to reddish grey; medium grained and contains more or less scattered large crystals of potassium feldspar. Granodiorites and quartz monzonites are the most common rock types in the Äspö diorite group but tonalites and quartz diorites are also included. Analysis of the Äspö diorite has given a well-defined age of 180463 million years.

The Småland granite differs from the Äspö diorite mainly by a higher amount of potassium feldspar and a brighter reddish colour.

Most of the greenstones are andesites to basalts and are probably supracrustal rocks incorporated in the rising magma. The greenstones occur as minor inclusions or irregular often elongated bodies following the E-W foliation trend.

The fine-grained granites are rich in quartz and potassium feldspar and they occur often as dikes. Brittle deformation in the granite have created many short joints lying closely together in contrast to the more widely spaced jointing in the medium to coarse grained granitoids. The most reliable age determination indicates that the age of the fine-grained granite is 1794 +16/-12 million years.

The numerically modelled parts of the tunnel system have a Äspö diorite content of approximately 95% of the volume. Hence, when modelling different tunnel areas the property of the Äspö diorite is used.



Figure 2-2. Compilation of the approximate rock distribution at different levels of the tunnel.

2.1.2 Tectonics

Several deformation zones of regional and local scale have been mapped in the Äspö area. Five of them will be discussed in more detail since they are located close to the tunnels. Of these five three are trending E-W and are named EW-1a, EW-1b and EW-3. The other two are trending N-E and are named NE-1 and NE-2.

These deformation zones make Äspö HRL located in a wedge with borders defined by EW-1b and NE-1. The HRL is further divided into one eastern part and one western part by NE-2. A top view of these zones is presented in Figure 2-3.

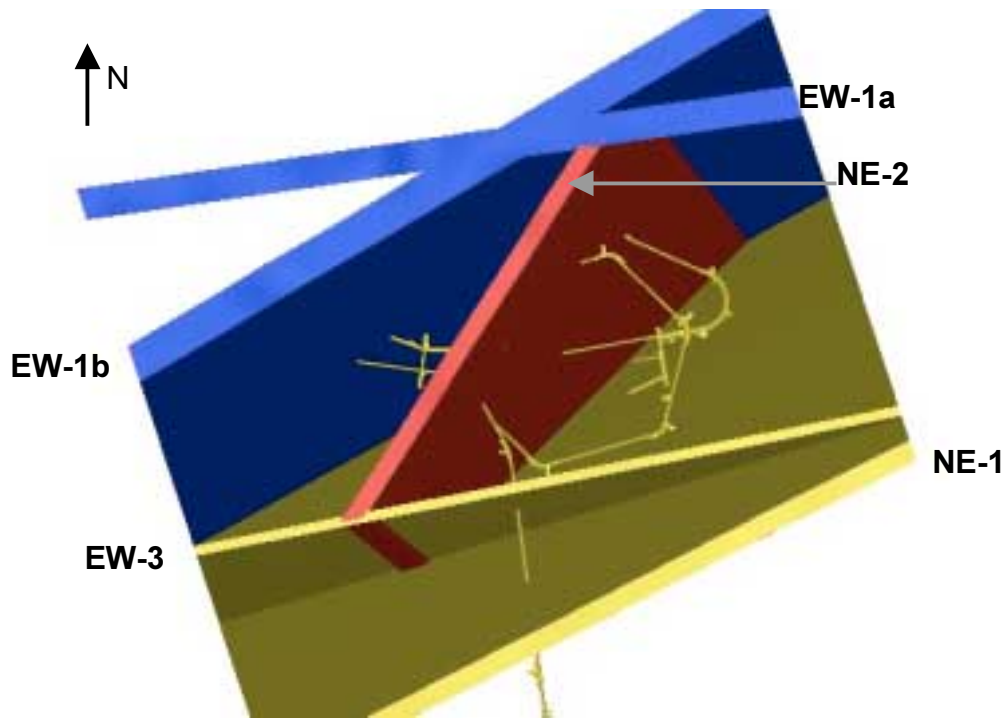


Figure 2-3. Top view of the larger deformation zones adjacent to Äspö HRL.

The dip in the text refers to the right hand rule. The zones in the figures look wider than mentioned in the text. Since the deformation zones are a bit undulating they are represented by a volume given a width that with a high level of confidence that enclose them. All strike directions are given in the Äspö 96 co-ordinate system in which North is 12 degrees West of true North, Figure 2-4.

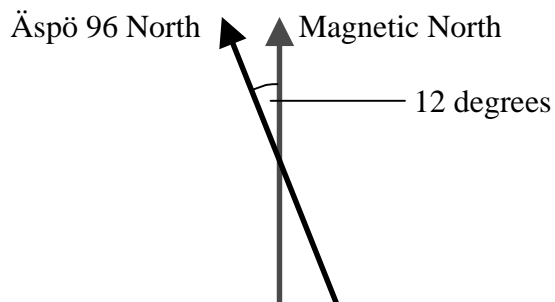


Figure 2-4. Äspö 96 north in relation to local magnetic north.

EW-1a and EW-1b

The thickness of the deformation zones EW-1a and EW-1b are approximately 50 m each and they were formed by early ductile/semi ductile deformation. Later brittle reactivation has also taken place. The strike/dip is 082/90 and 060/75 degrees respectively. The deformation zones, in relation to the tunnels, are shown in Figure 2-5.

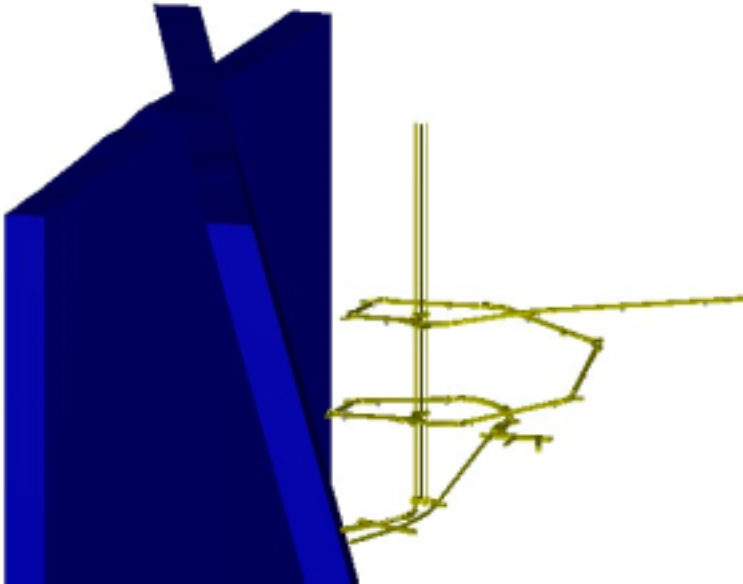


Figure 2-5. Location of the deformation zones EW-1a and EW-1b in relation to the tunnels, iso view.

EW-3

EW-3 has a 2–3 m wide crushed central section surrounded by 5–10 m of highly fractured Äspö diorite. The strike/dip is 079/79 degrees. The deformation zone is truncated against NE-1. EW-3's relation to the tunnels is shown in Figure 2-6.



Figure 2-6. Location of deformation zone EW-3 in relation to the tunnels, iso view.

NE-1

NE-1 is approximately 60 m wide, consisting of three branches. The northern branch is the most intense of the three branches and has an 8 m wide central part with centimetre wide open fractures and cavities. Another 10–15 m wide sections with more fractured rock on both sides surrounds the northern branch. The strike/dip is 243/70 degrees. NE-1's relation to the tunnels is shown in Figure 2-7.

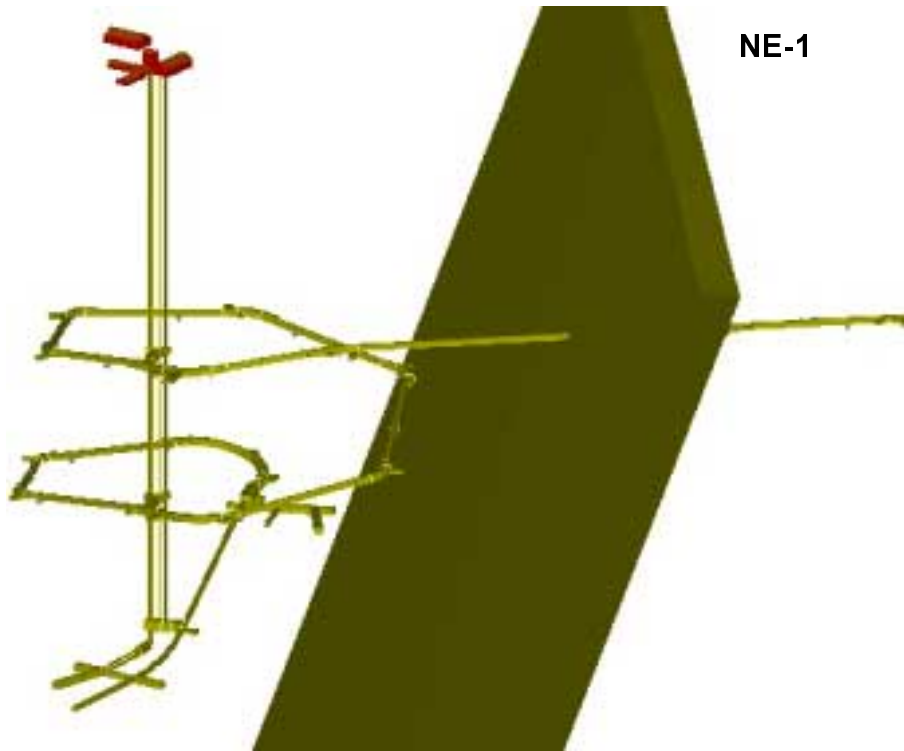


Figure 2-7. Location of deformation zone NE-1 in relation to the tunnels, iso view.

NE-2

NE-2 has a width varying between 1 and 5 meters where the centre is a brittle deformation influenced by a former ductile shearing and mylonitization. The strike/dip is 033/76 degrees. NE-2's relation to the tunnel is shown in Figure 2-8. The width of the deformation zone is decreasing with depth. In practice has the structure terminated below approximately 400 m in the Äspö tunnel.

The Äspö HRL is located in a wedge with borders defined by EW-1b and NE-1. The HRL is further divided into one eastern part and one western part by NE-2.

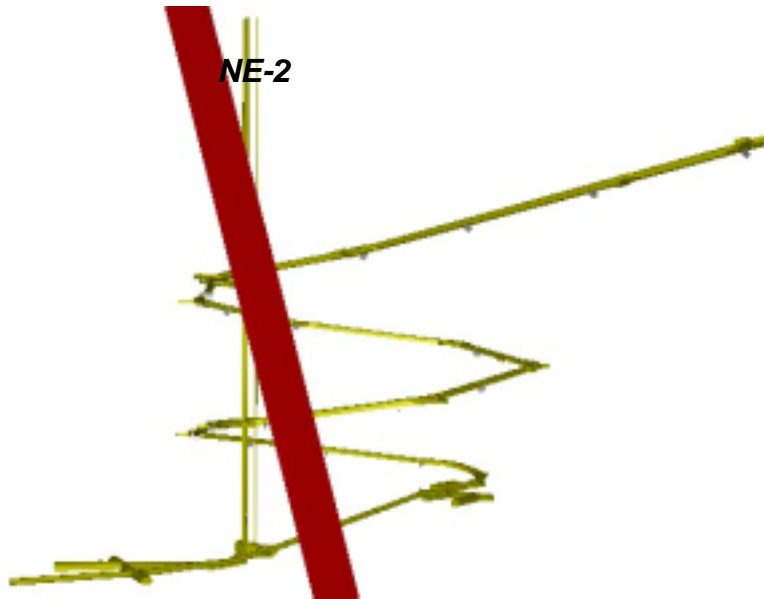


Figure 2-8. Location of deformation zone NE-2 in relation to the tunnels, iso view.

2.2 State of stress

Extensive rock stress measurement programs have been carried out at Äspö HRL. Locations of the stress measurements which results are presented in this section are shown in Figure 2-9.

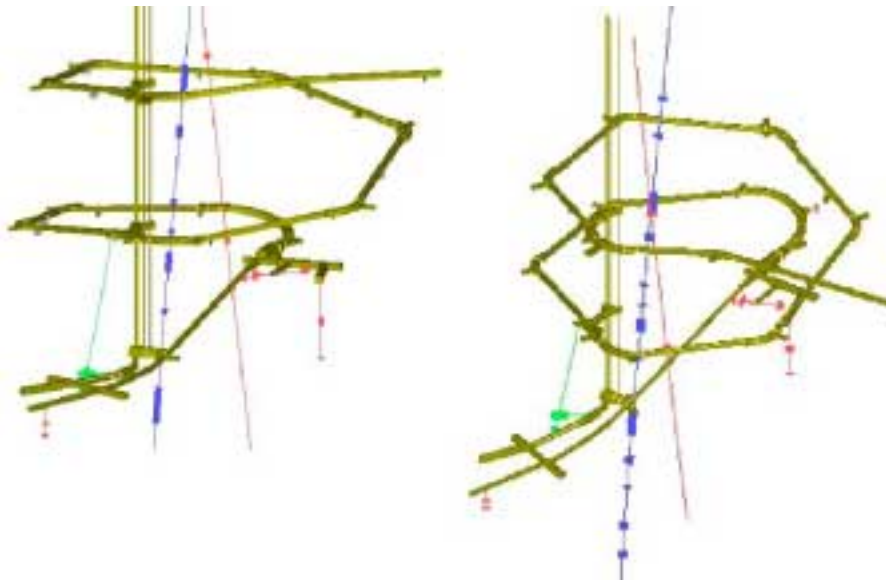


Figure 2-9. Location of performed stress measurements indicated by thick markers. Red markers – overcoring, Blue markers – hydraulic fracturing, Green markers – both hydraulic fracturing and overcoring.

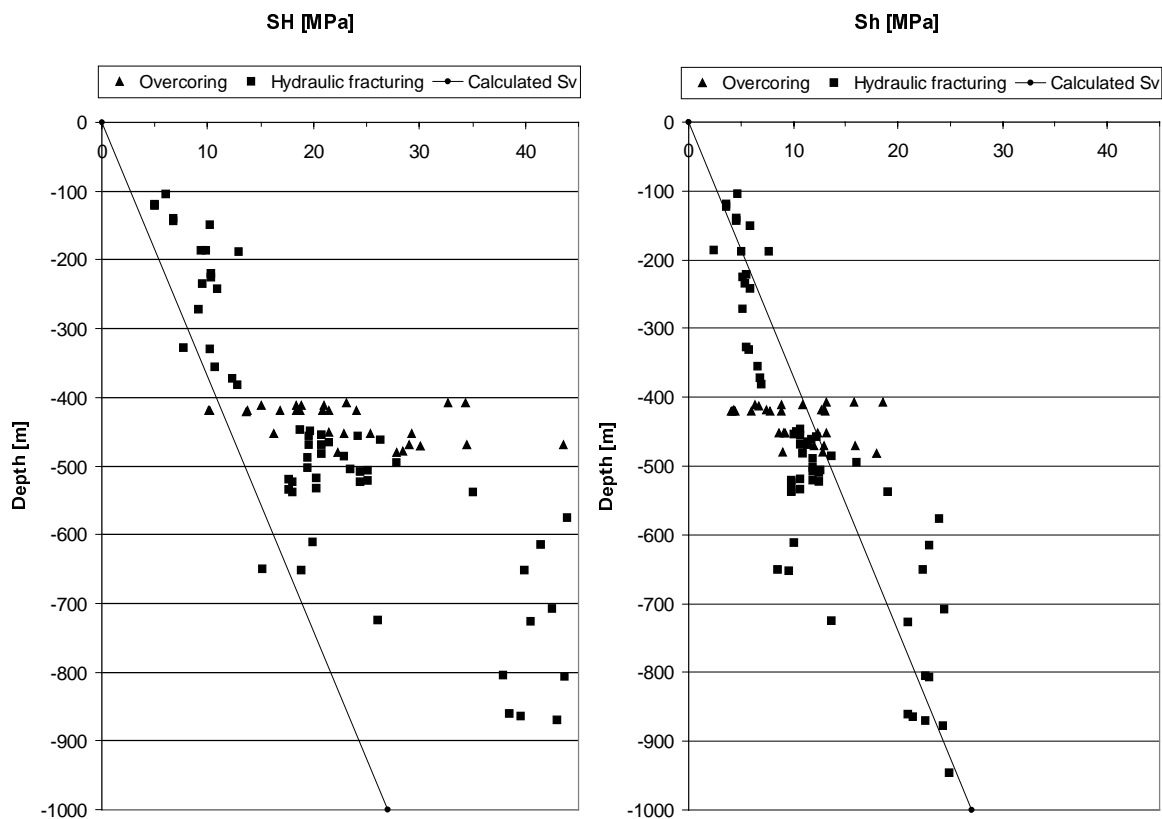


Figure 2-10. Major and minor measured horizontal stresses at Äspö HRL at different depths.

Stress measurement results from 2D and 3D overcorings as well as hydrofracturing tests are presented in Figure 2-10. The results are presented as the major and minor horizontal stresses.

The measured bearings for the horizontal stresses are presented in Figures 2-11 and 2-12. The results originate from both the overcoring and hydraulic fracturing techniques. The average bearing used for the numerical modelling is included as a vertical line in Figure 2-11.

At 400–500 m depth measurements indicates a sudden increase of the stress magnitudes. The reason for this has not yet been explained. One possible explanation is occurrence of horizontal mylonite zones but this has not yet been validated /Ask, 2001/.

Earlier rock stress measurements indicate that the minor principal stress component's bearing changes from vertical to a dip more horizontal than the intermediate principal stress. Hence, the vertical stress becomes higher than the minor horizontal stress. Figure 2-13 is based on Makurat et al. /2002/ and shows regression lines for the average measured minor horizontal and vertical stresses in relation to the theoretical vertical stress using the density 2.7 g/cm^3 . Results from both overcoring and hydraulic fracturing have been used. Recent rock stress measurements by hydrofracturing performed in October 2001 gives the same indication, Rummel et al. /2002/. These observations are also supported by the fact that the most conductive fractures in the HRL are parallel to the major principal stress. If the intermediate stress component is steeper dipping than the minor stress component the fractures parallel to the major principal stress will be opened instead of closed by the rock stresses. A rose diagram showing the direction of the water bearing fractures in TASF is presented in Figure 2-14. The average dip for the presented fractures is 80 degrees from horizontal.

SH Bearing [Degrees E of N]

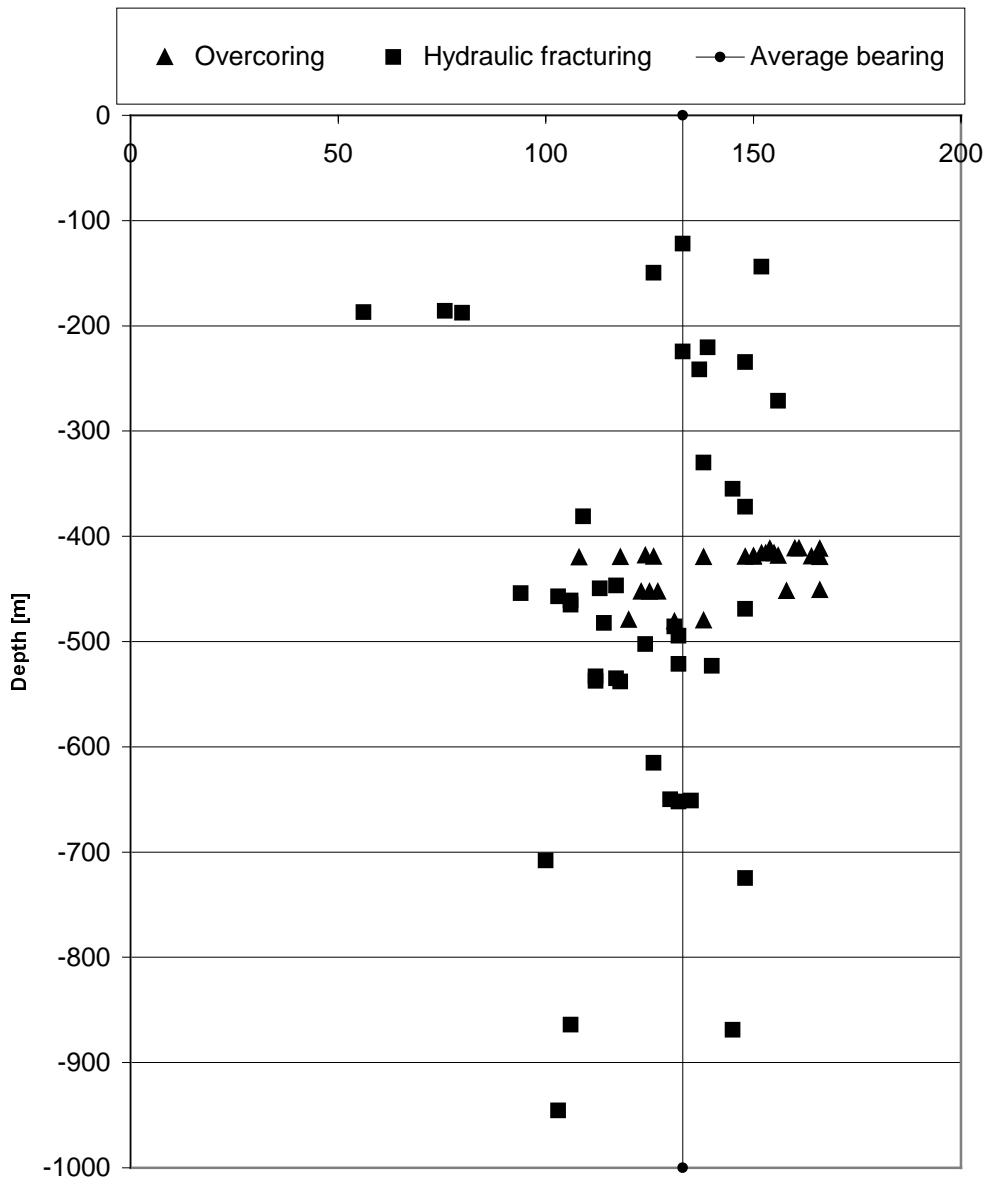


Figure 2-11. Bearing of measured maximum horizontal stresses at Äspö HRL at different depths including the average bearing used for the numerical modelling (vertical line).

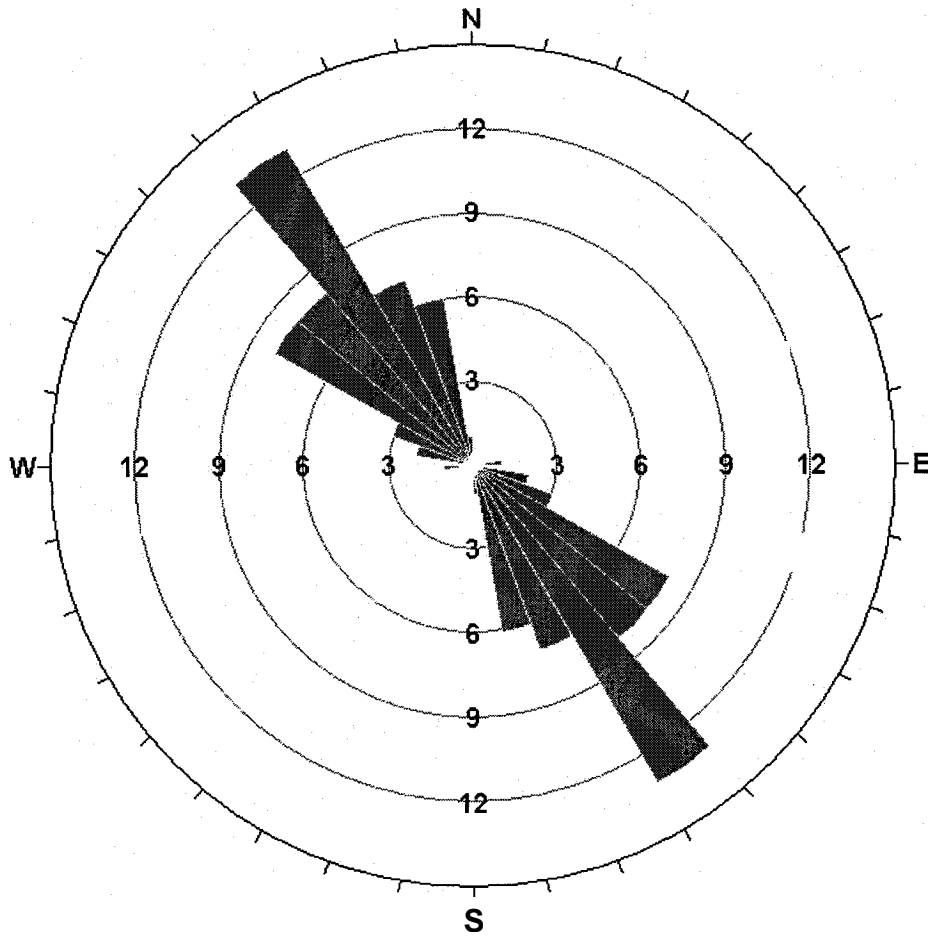


Figure 2-12. Rose diagram of maximum principal stress orientation. Data from hydrofracture tests in borehole KAS02 and mean values from all overcoring tests /Makurat et al., 2002/.

The mean values of rock stress measurement results from the boreholes closest to the areas modelled have been used in numerical model. Only overcoring measurements have been used in order to get a three-dimensional stress tensor. The derived stress tensors for the 420 m and 450 m levels are presented in Table 2-1. Average values for the minor horizontal stress achieved from recently made hydraulic fracturing tests in the area is included for comparison /Rummel et al., 2002/.

Table 2-1. The three-dimensional stress tensor for the 420 and 450 m levels used for numerical modelling. Results from hydraulic fracturing added for comparison.

	σ_1 (Mpa)	σ_2 (Mpa)	σ_3 (Mpa)	σ_h (Mpa)
Magnitude 420 m	27	17	9	
Magnitude 450 m	29	21	10	11
Trend (degrees)	133	49	234	130
Plunge (degrees)	19	42	33	

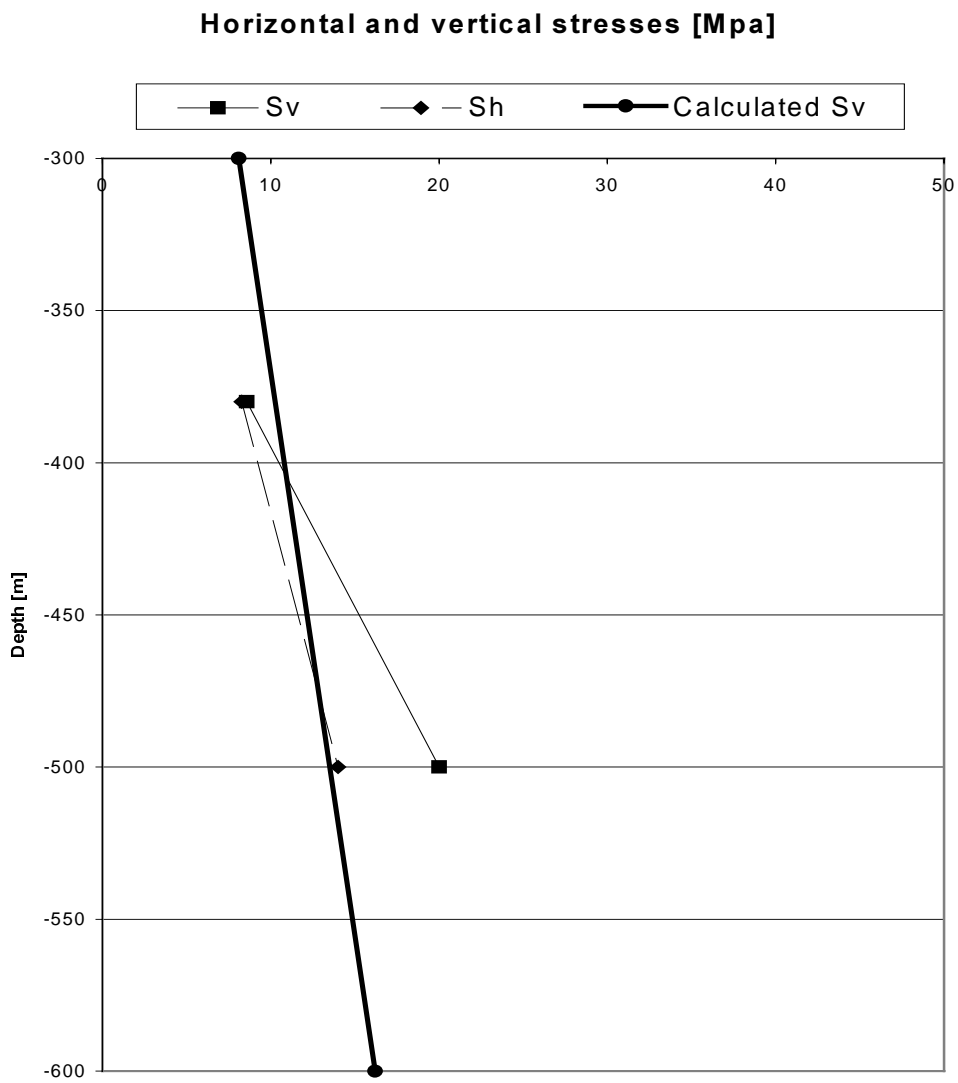


Figure 2-13. Regression lines for the measured minor horizontal and vertical stresses in relation to the theoretical vertical stress. Makurat /2002/.

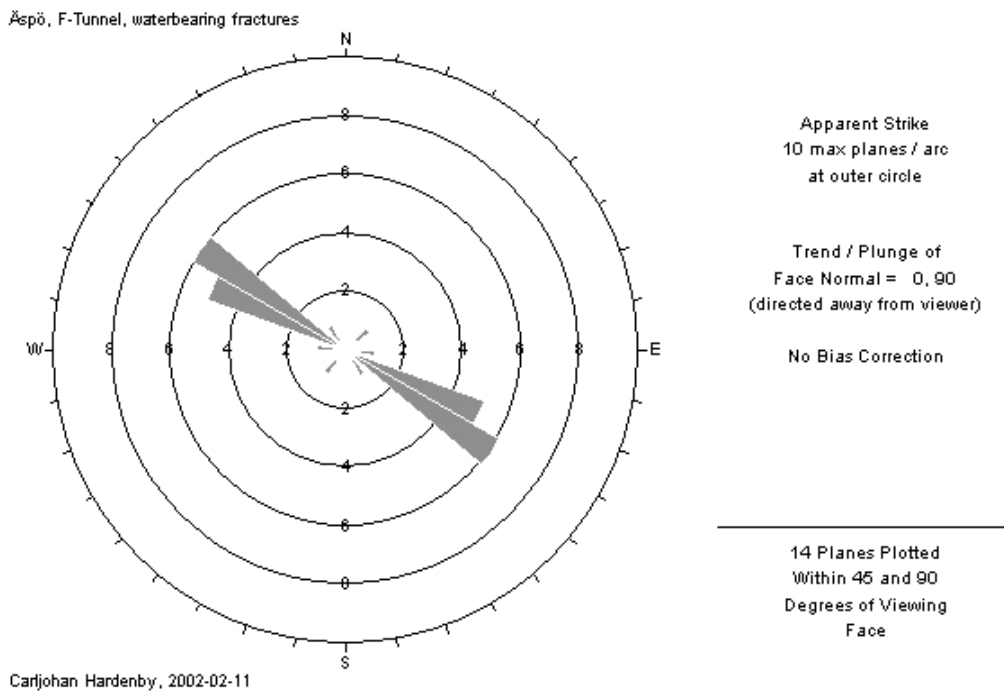


Figure 2-14. Rose diagram showing the direction of the waterbearing fractures. The fractures have an average dip of 80 degrees from horizontal. Note that the strike is related to magnetic north.

2.3 Site layout

Information about the design and construction of the Äspö HRL is derived from Hedman /1999/. The entrance to the tunnel is located near the Oskarshamn nuclear power plant at the Simpevarp peninsula. After the first 1600 m the ramp reaches Äspö at a depth of 200 m. The ramp continues in a hexagonal spiral and completes its first turn at 340 m. The spiral continues to a depth of approximately 390 m where a sharp turn is made. This deviation from the original spiral is made to make sure that the regional zone NE-1 not is passed a second time. In the first place the layout was chosen to study NE-1. It was though so problematic to pass the deformation zone the first time that the tunnel layout was changed later on. After the sharp turn the tunnel is curved slightly to the right before it ends at 450 m depth. After completion of the main tunnel the side tunnels for different kinds of experiments and installations were excavated.

2.3.1 Tunnel dimensions

The tunnel should be able to host vehicles with a height and width profile of 3.5 respective 3.0 m. The section chosen was a 25 m² 5 m wide cross sectional area down to 340 m. It was there narrowed down to a width of 4.8 m since there are less rack for installations in that part of the tunnel. In curves and passing places the tunnel has been widened to 8 m which gives a cross sectional area of 42 m². Figure 2-15 illustrate the tunnel profiles in the curves and the straight part of the ramp.

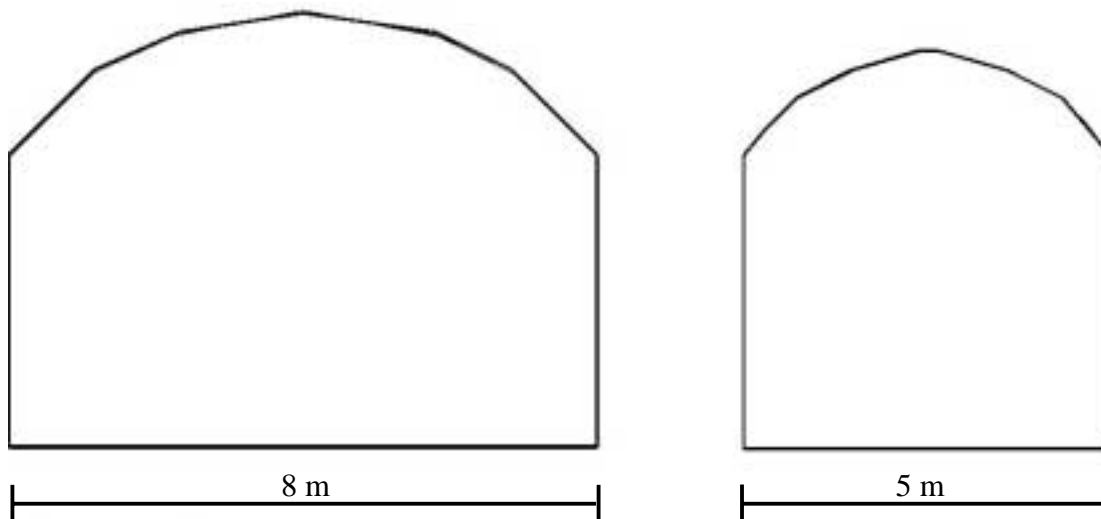


Figure 2-15. Drawing of the 42 m² tunnel profile to the left and the 25 m² tunnel profile to the right.

Curve radii are normally 20 m except for the long curve at -390 m where a radius of 40 m is used.

The inclination of the tunnel is 0.140 levelling out to 0.100 in the curves. From the second turn of the spiral the inclination of the curves was also set to 0.140.

2.4 Construction

Conventional drill and blast technique was used down to 420 m or 3100 m along the ramp. At this level a larger cavern was built. In the cavern the TBM-machine that was used to bore the last part of the tunnel down to 450 m was assembled.

Two air supply shafts with a diameter of 1.5 m each and one hoist shaft with a diameter of 3.8 m was raise-bored from the Äspö island intersecting the tunnel at 220, 340, and 450 m depth.

The construction work began 1990 and the drill and blast tunnelling including the cavern at the 420 m level was finished in April 1994. The TBM tunnelling commenced in mid June -94 and was finished in mid September the same year. Additional excavations at various areas completed the rock excavation work in the beginning of 1995. Final installations of the water drainage system and the hoist were completed during the summer of 1995.

2.4.1 Rock support and grouting

Ordinary Swedish support and grouting techniques were used during construction. Rock bolts, shotcrete with and without steel fibres and shotcrete arches were used for support. For grouting cement and polyurethane based grouts were used.

The overall strategy for support and grouting was that it should be performed to a very limited extent. The geohydrology should be disturbed as little as possible and researchers should be able to go back and study the exposed rock surfaces. All support and grouting actions were therefore discussed with, and agreed upon by the SKB representatives.

3 Maintenance

To isolate areas in the tunnels where more rock maintenance than average has been carried out two different methods have been used. First an interview with one of the miners performing scaling and bolting in the tunnels was held. After that the records for bolting and shotcreting were studied.

3.1 Interview

The interview was conducted with Nilsson /2000/, who has been working with maintenance/scaling since the autumn of 1998. Nilsson pointed out that the following parts of the tunnel needed repeated maintenance.

1. NASA 3009A, -400 m
This niche has been scaled several times. At one scaling occasion noise from microseismic events was heard. Most of the scaling was done in the niche's front. The niche was later stabilised with fibre-reinforced shotcrete in the roof and the upper part of the front.
2. NASJ 0015B, -450 m
Repeated scaling
3. T ASD, -420 m
Scaling at several occasions in the tunnel front and right wall. Noise from microseismic events heard.
4. T ASO, -420 m
Some rock fragments fell from the roof during a backfill-packing test performed in this tunnel. Additional scaling was then performed. Noise from microseismic events was heard during scaling.
5. T ASF, -450 m
This side-tunnel has been scaled once a month since 1998. Approximately the same volume was scaled each month. Most of the scaling was done in the roof.
6. T ASJ and its crossing with T ASA and T ASI, -450 m
The roof have been bolted since it had to be scaled quite frequently.

The location of these areas in the tunnels is illustrated in Figure 3-1.

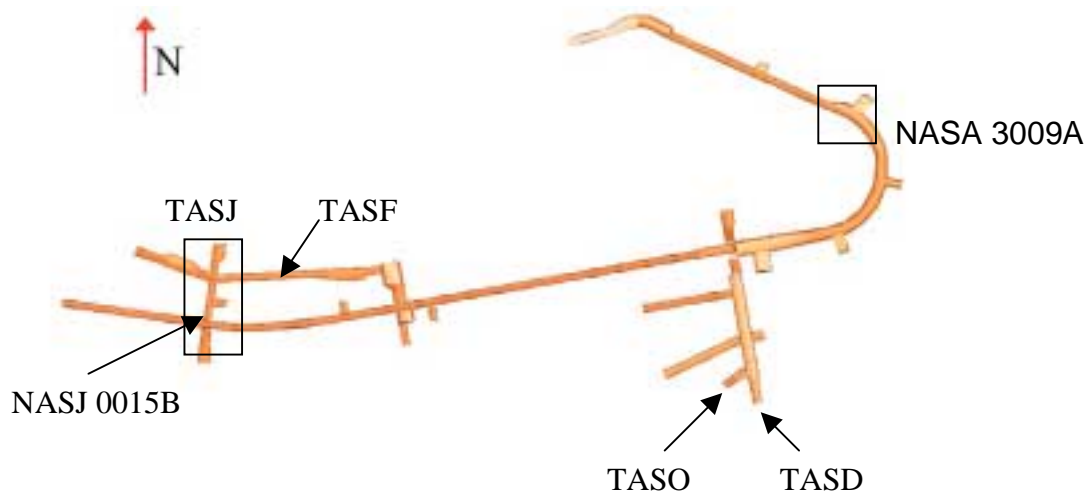


Figure 3-1. Areas in the tunnels needing additional maintenance according to interview.

3.2 Maintenance records

To investigate the long-term behaviour of the main tunnel three different parameters were derived from the records, the amount of: scaling, shotcreting and bolting. The parameters were sorted into nine different groups. Each group is representing a leg of the hexagonal spiral down to approximately 390 m.

Only data from below a depth of approximately 200 m and downwards were used since it was assessed that the rock stresses above this level are too small to create stress corrosion.

3.2.1 Rock mass quality

During the excavation phase the tunnel front was geologically mapped and RMR classified after each round. The major part of the tunnel is classified as good rock with an RMR-value ranging between 60 to 80. Two legs of the studied part of the tunnel have been classified as fair with RMR values between 40 to 60. These parts together with the location of the nine different legs studied are presented in Figure 3-2. Each leg begins at the start of the upstream curve and terminates at the beginning of the downstream curve.

The chainage for the legs are presented in Table 3-1. The chainage starts at the tunnel entrance.

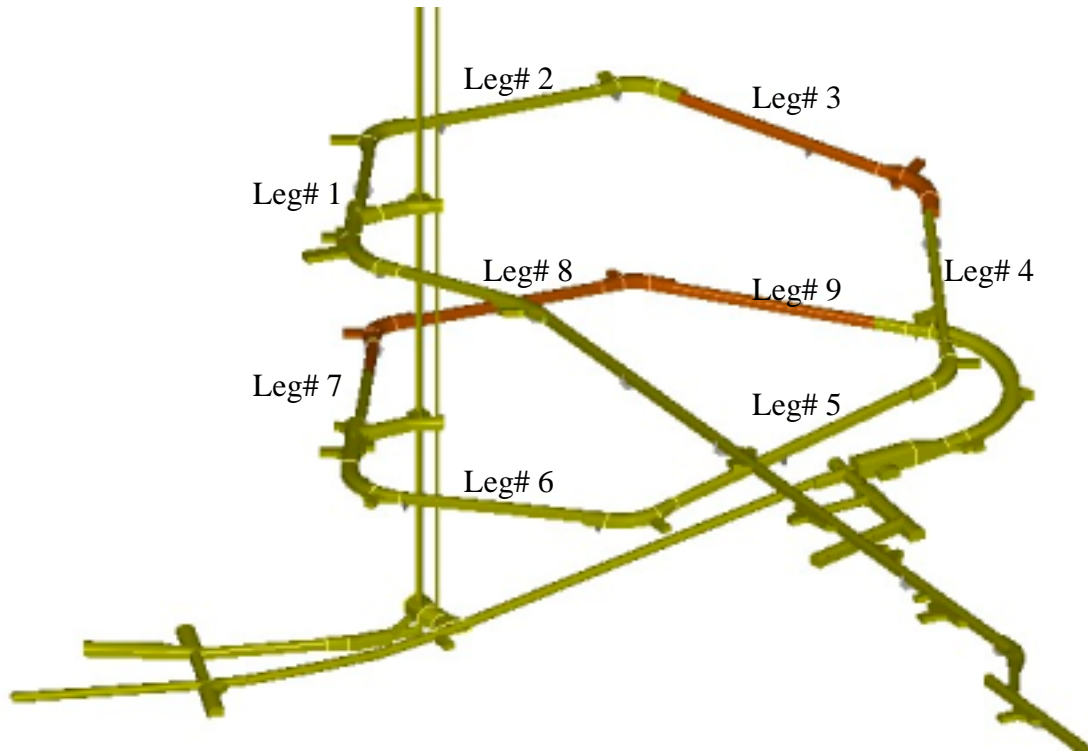


Figure 3-2. The nine different tunnel legs and the parts of the tunnel classified as fair rock (RMR 40–60) coloured red. The rest of the tunnel within the legs is classified as good rock (RMR 60–80).

Table 3-1. Chainage for the different legs presented in Figure 3-2.

Leg #	From section (m)	To section (m)	Angle relative σ_1 trending 133°
1	1584	1745	65
2	1745	1883	60
3	1883	2028	0
4	2028	2178	55
5	2178	2357	60
6	2357	2496	0
7	2496	2699	65
8	2699	2840	60
9	2840	2997	20

3.2.2 Scaling, bolting and shotcreting

Scaling is represented in the database as a total volumetric value for a section scaled a certain period of time. Bolting is presented as number of bolts within a certain section and shotcreting as shotcreted sections. To handle the sometimes-overlapping records for each parameter the total volume/amount/length for one leg was added and then divided with the total length of each leg. When normalising the parameters like this each leg can be compared with any of the others although they have a somewhat different length.

In the records only scaling performed after the excavation phase are stored. For the bolting and shotcreting though, there are a complete records over time. These records have therefore been separated to “excavation phase” and “operational phase” groups. Time dependent deterioration in parts if the tunnel should stand out more explicitly when the parameters are separated in time.

Relation of tunnel angle to major principal stress

The angle between each tunnel leg and the major principal stress effects the stress situation around the tunnel and could impact on the need for additional scaling or other maintenance activities. The angles for the different legs have therefore been derived and are presented with the other data. The angle between the legs and the major principal stress are very similar between most of the legs. They were therefore divided into two groups where the first group are legs with an angle of 0 to 20 degrees and the second group legs with an angle of 30 to 65 degrees to the to the major principal stress.

Relation to water inflow

Since the operational phase began the water flow for each tunnel leg has been constantly measured in a number of weirs. The flow data have been compared with the data from the other records.

3.2.3 Compilation of scaling, bolting and shotcreting records

The relation between scaling, bolting and shotcreting together with the leg’s angle to the major principal stress is presented in Figure 3-3. The legs are presented in the two groups they were divided into regarding their angle relative the major principal stress. The geological mapping presented in Markström /1996/ has been used as a reference when the geology at different areas is discussed.

All of the bolting in leg# 1 has been done in the last part of the widened curve from 1620–1680 m down the ramp. The geology there is a mixture of Äspö diorite, Greenstone, Fine-grained granite and some Pegmatite. No increased fracturing is mapped. The shotcreting have been done in the same area. The major part of the scaling has been done from 1650–1680 m down the ramp.

The bolting and shotcreting in leg# 2 have been done in the widened curve from 1750–1780 m down the tunnel. The geology consists of rather homogeneous Äspö diorite with a thin mylonite zone following the tunnel in the roof. Approximately 65% of the scaling have been performed from 1820–1883m. Half of this length consists of Småland granite and the other half of Äspö diorite, both with veins of Fine-grained granite. The part with Småland granite includes some smaller fracture zones along the roof.

In leg#3 the bolting has been done partly in a contact between Småland granite and Fine-grained granite and partly in homogenous Äspö diorite. The bolting is located in a fracture zone. The scaling volumes are very evenly distributed along the leg.

In leg# 4 75% of the shotcreting have been done from 2120–2178m down the ramp. Half of this shotcreted length has covered homogenous Småland granite and the rest an area of Äspö diorite with veins of Fine-grained granite. The scaling volumes are very evenly distributed along the leg.

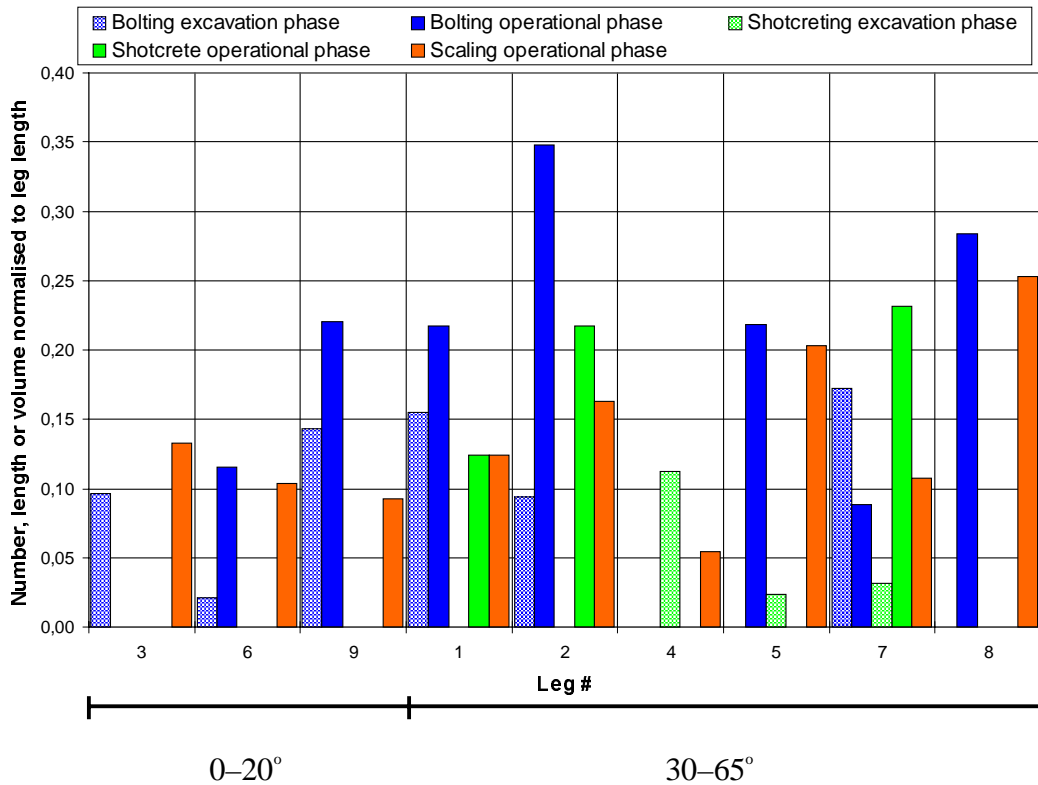


Figure 3-3. Compilation of records for scaling, bolting and shotcreting for the different tunnel legs and their relation to the major principal stress.

The four meters of shotcreting in leg# 5 is a continuation of the shotcreting in leg# 4, hence in the curve between the legs. The bolting in leg# 5 has been done from 2325–2355m down the ramp in a Äspö diorite area with veins of Fine-grained granite. The scaling are rather evenly distributed but concentrated around veins of Fine-grained granite.

Most of the bolting in leg# 6 has been done where the tunnel widens up and the curve begins from 2360–2380 m down the ramp. The geology is a continuation of the one described in leg# 5. The scaling is rather evenly distributed with some increase where the curve ends and the tunnel is narrowed down.

The bolting during construction in leg#7 has been done in an area of fractured Fine-grained granite where the tunnel narrows down after a curve. During the operational phase the bolting has been performed in a normally fractured Äspö diorite area close to the Fine-grained granite. These two bolted areas from 2570–2610 m down the ramp where later covered with shotcrete. Half of the scaling is concentrated to two locations and the rest distributed along the leg. The scaling concentrations are at 2490–2510 m and 2621–2660 m down the ramp. The first concentration is in Äspö diorite with small intrusions of Fine-grained granite. The second concentration is in Äspö diorite and Småland granite.

All of the bolting in leg# 8 has been performed from 2710–2735m down the ramp in the widened part of a curve. The area is generally increased fractured and includes one minor fracture zone. The scaling is evenly distributed and most of the leg consists of Småland granite with increased fracturing.

Leg# 9 has been bolted in two different areas. The first from 2860–2870 m down the ramp in the widened part in the middle of one curve. The geology is a mix of Äspö diorite and Fine-grained granite. The second bolted part is from 2900–2940 m down the ramp. 2900–2910 m is an area of Småland granite with a larger intrusion of Fine-grained granite covering the major part of the roof. The rest of the bolted area includes a 10 m fracture zone. The rock-type is Äspö diorite with one vein of Fine-grained granite. The scaling has been done from 2860–2900 m and from 2970–3000 m. The first part has the same geology as the curve mentioned above and the second part consists only of Småland granite.

3.2.4 Compilation of water inflow records

In addition to geology the water inflow records were also studied. The relation between scaling and water inflow together with the leg’s angle to the major principal stress is presented in Figure 3-4. Four of the legs have a significant larger inflow compared to the other legs and one leg has a much lower inflow.

When studying the water inflow records for the operational phase there is a remarkable uniform decrease in almost all of the weirs. Figure 3-5 is a compilation of the average water flow from October to December through the weirs from 1995 to 2000. The legend “MA****” below the X-axis means Measurement in the main tunnel (TASA) and the numbers indicates the chainage. The weirs from MA0682G to MA3179G are located in the spiral. The rest of the boxes are located in the TBM-tunnel except for MF0061G that is located in the TASF-tunnel.

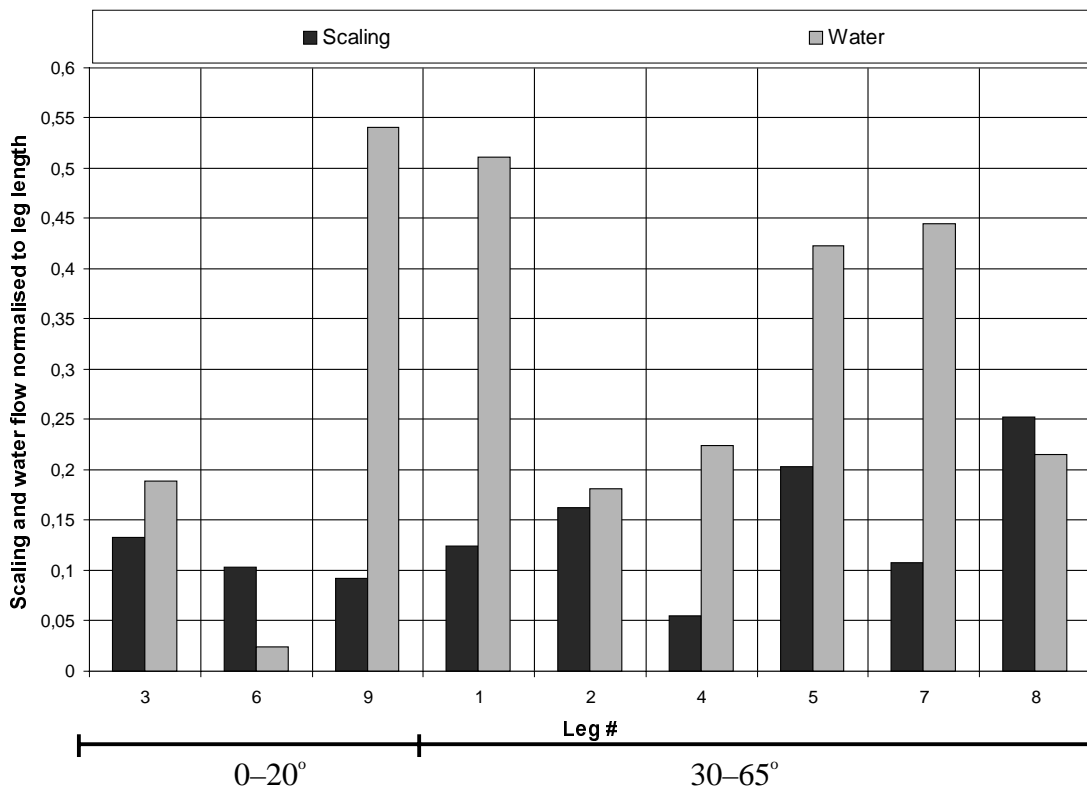


Figure 3-4. Compilation of records for scaling and water inflow for the different tunnel legs and their relation to the major principal stress.

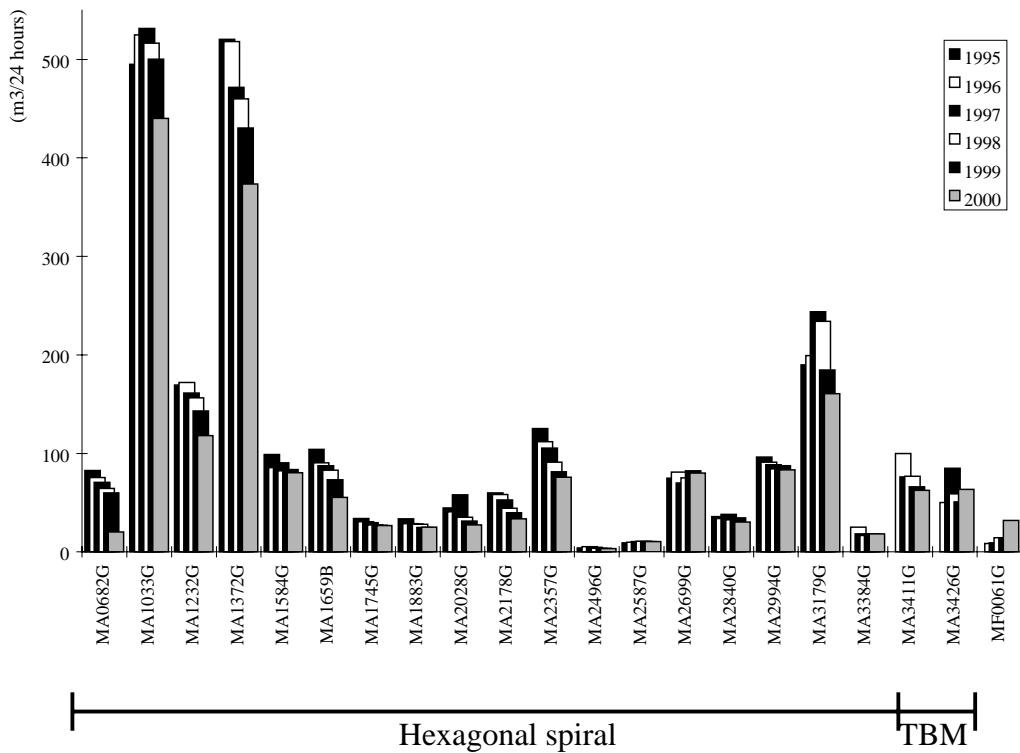


Figure 3-5. Average water flow through the weirs during five years. The measurements are made from October to December each year.

When looking at the total water flow in the tunnel the decrease from 1995 to 2000 is 22% or 4.4% per year. The average daily flow from October to December through the tunnel and the decrease for each year is presented in Table 3-2.

Table 3-2. Total water flow through the tunnel from October to December.

Year	Water flow (m ³ /24h)	Decrease (m ³ /24h)	Decrease (%)	Decrease since 1995 (%)
1995	2479			
1996	2438	41	1.7	1.7
1997	2393	45	1.8	3.5
1998	2268	125	5.2	8.5
1999	2105	163	7.2	15.1
2000	1930	175	8.3	22.1

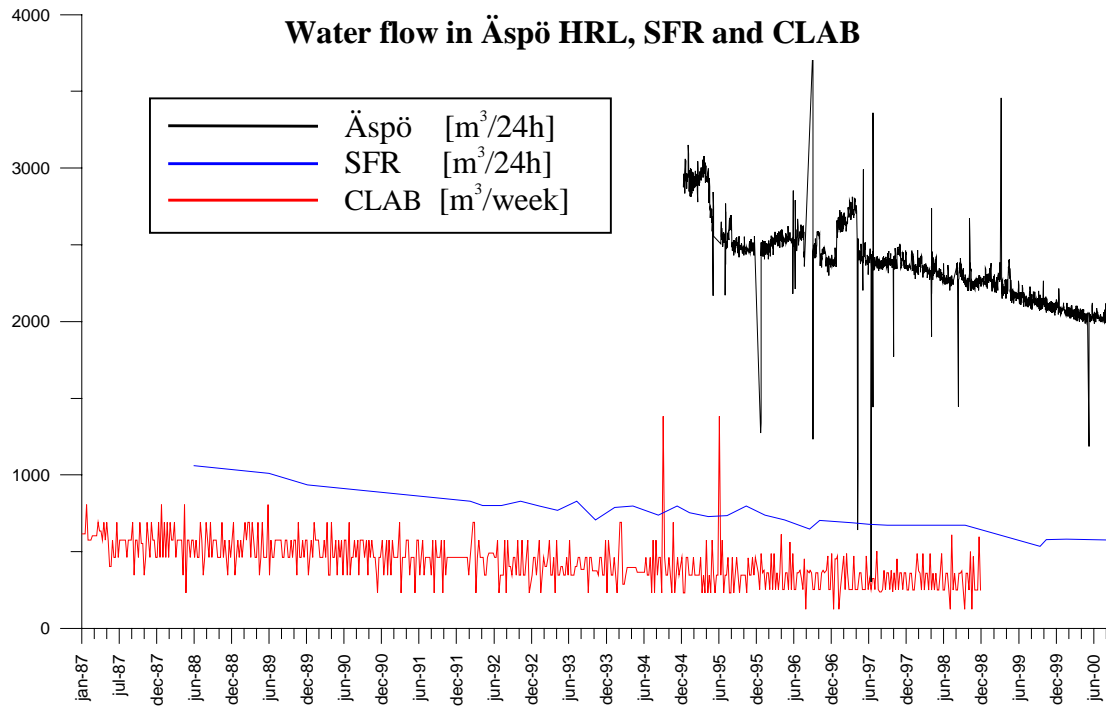


Figure 3-6. A comparison of the water flow rates and its decrease at Äspö HRL, SFR and CLAB.

SKB is responsible for two other rock cavern facilities, CLAB and SFR. CLAB is the interim storage for the spent nuclear fuel and different reactor components that will be placed in a deep repository. The facility is located approximately 5 km from Äspö HRL in the Simpevarp peninsula. SFR is the final storage for low and intermediate active waste from nuclear power stations, hospitals and other facilities producing contaminated waste. SFR is located close to the Forsmark nuclear power station approximately 170 km north of Stockholm. The water flow in these facilities has also been monitored for a quite long period of time and the trend of decreasing inflow is also found here. A comparison of the water flow in the three different facilities is presented in Figure 3-6.

The water flow in SFR has decreased approximately 45% or 3.8% per year during its 12 years of operation. The same numbers also apply for the CLAB facility.

3.3 Maintenance in TBM and D&B tunnels

Äspö HRL offers a unique possibility to compare the need for maintenance in TBM and drill and blast tunnels. At 450 m depth the bored part of the main tunnel lies parallel to a D&B tunnel (TASF) only 27m apart, see Figure 3-7. The geology is almost identical in the TBM tunnel and the first half of TASF. The TASF-tunnel though, has some fine-grained granite areas in the first half. The second half of TASF is excavated in Småland granite, which is more brittle than the Äspö diorite in its first half. The scaling record indicates a rather uniform scaling volume for the different parts of the tunnel. When normalising the TASF records using the same principle as with the tunnel legs the normalised scaling for TASF is 0.5 and the normalised bolting 0.25. During the winter

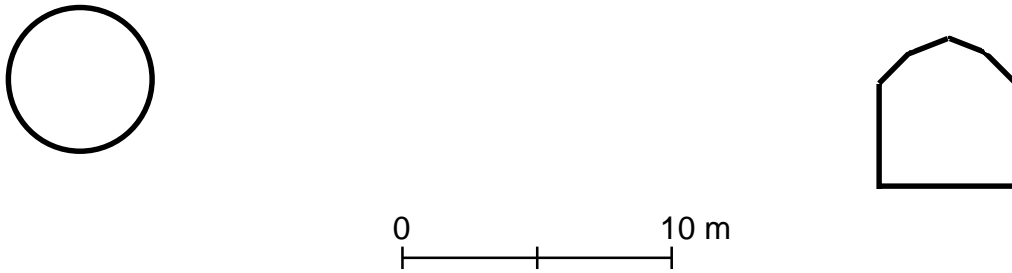


Figure 3-7. Section of TASF and the TBM-tunnels relative location.

of 2001 the roof in the whole tunnel was shotcreted. For the entire TBM tunnel no maintenance at all has been performed. Excepted are areas where side tunnels or niches are located.

4 Numerical modelling

The numerical modelling was carried out using the three-dimensional boundary element program Examine3D™ available from Rocscience Inc. The following types of analysis parameters were selected. Linear elements, where nodes are shared by neighbouring triangular elements. Mixed integration mode in which both numerical and exact integration is used. The matrix solver was set to “generalised minimum residual”.

The Mohr-Coulomb failure criterion with the parameters presented in Table 4-1 was used:

Table 4-1. Rock mechanics parameters used for the numerical modelling.

Parameter	Value
Young's modulus	40 000 MPa
Poisson's ratio	0.2
Tensile strength	10 MPa
Cohesion	35 MPa
Friction angle	35 degrees

Since only stresses have been modelled the parameter values presented above will not impact on the results.

The in situ stresses used for the numerical modelling are presented in Table 2-1.

The element size in the modelled areas was set to 0.3–0.4 m. Comparisons with the exact simple Kirsch solution for a circular tunnel gave an average error of 5% in the immediate vicinity of the excavation. The error is less than 2% from a radial distance of 0.1 m from the excavation. The field point grid around the modelled areas had a spacing of 0.25 m in all three dimensions. There is though one exception in the modelling of NASJ. To be able to run the model the grid had to be changed to a spacing of approximately 0.31 m.

4.1 Strategy

Stability issues around underground openings can be grouped as either /Martin et al., 2001/:

1. Gravity driven wedge type failures usually associated with regions of low confinement, $\sigma_3 \approx 0$ or
2. Stress induced spalling caused by tangential stress concentrations on the boundary of the opening. Using a Damage Index (D_i) for circular openings expressed as:

$$D_i = \frac{3\sigma_1 - \sigma_3}{\sigma_{ci}} = \frac{\sigma_{\max}}{\sigma_{ci}} \quad (4-1)$$

where σ_1 and σ_3 are the far-field principal stresses in the plane of interest and σ_{ci} is the laboratory uniaxial compressive strength. Martin et al. /2001/ found that when $D_i \geq 0.4$ stress induced spalling was evident. σ_{\max} in equation (4-1) can be determined from numerical models when the tunnel is not circular. The two modes of instability and the Damage Index associated to them is presented in Figure 4-1.



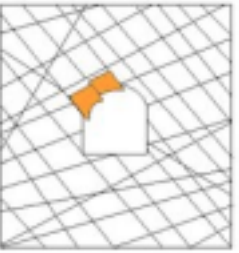





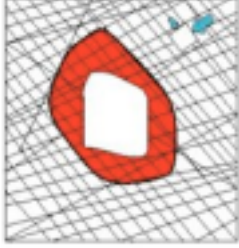
	Massive ($GSI > 75$)	Moderately Fractured ($50 > GSI < 75$)	Highly Fractured ($GSI < 50$)	
Low In-Situ Stress ($\sigma_1 / \sigma_c < 0.15$)	 Linear elastic response.	 Falling or sliding of blocks and wedges.	 Unravelling of blocks from the excavation surface.	$D_i < 0.4 (\pm 0.1)$
Intermediate In-Situ Stress ($0.15 < \sigma_1 / \sigma_c < 0.4$)	 Brittle failure adjacent to excavation boundary.	 Localized brittle failure of intact rock and movement of blocks.	 Localized brittle failure of intact rock and unravelling along discontinuities.	$0.4 (\pm 0.1) > D_i < 1.1 (\pm 0.1)$
High In-Situ Stress ($\sigma_1 / \sigma_c > 0.4$)	 Failure Zone Brittle failure around the excavation.	 Brittle failure of intact rock around the excavation and movement of blocks.	 Squeezing and swelling rocks. Elastic/plastic continuum.	$D_i > 1.1 (\pm 0.1)$

Figure 4-1. Tunnel instability and modes of failure. The Damage Index D_i is defined as the ratio of maximum tangential stress on the boundary of the tunnel (σ_{\max}) to the uniaxial compressive strength σ_c /Martin et al., 2001/.

Martin et al. /2001/ also suggested that when the far-field stresses are such that $Di \geq 0.4$ the depth of spalling-type failure can be estimated by a simple deviatoric stress criterion given by: $\sigma_1 - \sigma_3 > k\sigma_{ci}$ where K is determined from back analysis of existing failures. Where failure has not occurred Martin et al. /1999/ suggested that K be assigned a value of 1/3. In this report the K -values were chosen such that $K\sigma_{ci}$ ranged from 50 to 70 MPa. This implies that for a Mohr-Coloumb failure criterion the rock mass should be close to spalling-induced failure when the uniaxial strength of 50 to 70 MPa is exceeded (assuming $\phi=0$, i.e., not mobilized).

In order to validate the results of the numerical modelling, photographs of the modelled areas were taken. Scaling or bolting visible in the photographs could then directly be compared with the modelling results. Some of the photographs show areas with a lot of rock support. The support, in these cases, has been installed to ensure that damage does not occur to an ongoing experiment and to ensure adequate safety for workers.

4.2 Areas with significant maintenance records

All the areas referred to in the interview in section 3.1 were selected for further numerical modelling. No numerical modelling was performed on any of the nine legs since the records did not support the idea that stress-induced spalling was occurring in the main tunnel legs. Two additional locations were added to the list of areas to be numerically modelled. The first location is a part of the TBM tunnel for the comparison of the TBM and D&B tunnels. The second location was added after a diesel driven compressor was placed in niche NASA 3419B at -450 m. The increased heat in the roof (approximately 50 degrees C) of the niche and the associated thermal expansion had the effect that a lot of smaller rock fragments had to be scaled from the roof. Scaling was performed in the niche two years prior to the installation of the compressor. The niche was chosen for modelling because it appeared that stress magnitudes were sufficiently large that with the increased thermally-induced stresses the rock appeared to spall. It was therefore of interest to have a better idea of the initial stress magnitudes before heating took place. A summary of the areas that were numerically modelled is presented in Table 4-2 and Figure 4-2. The table also includes a brief maintenance summary as well as the damage index according to equation (4-1). A rock mass UCS of 180 MPa and a numerically calculated σ_{max} have been used to derive the damage index.

As can be seen in the table all of the more problematic areas have a Damage Index that indicates that stress induced spalling is close at hand.

Table 4-2. Summary of the numerically modelled areas, their maintenance and Damage Index (numerically calculated σ_{max} used).

Area	Maintenance summary (activity: YY-MM)	σ_{max} (Mpa)	Di
1. NASA 3009A	Scaling: 98-11 and 99-01	70	0.39
2. T ASD	Scaling: 99-04, 99-09 and 00-01 Bolting: 97-07 and 97-09	75	0.42
3. T ASO	Scaling 98-03, microseismic events then heard	40	0.22
4. NASA 3419B	Scaling: 99-02 and 01-01. Microseismic events heard once	70	0.39
5. NASJ 0015B	Scaling: 98-03	70	0.39
6. T ASJ and its crossing with T ASA and T ASI	Scaling: 98-09, 99-04 and 99-10	100	0.56
7. T ASF	Scaling: 95-05, 97-05, 98-05, 99-04, 99-10 and 00-09 Bolting: 95-03, 98-06 and 01-01	50	0.28
8. T ASA adjacent to T ASF	No maintenance	50	0.28

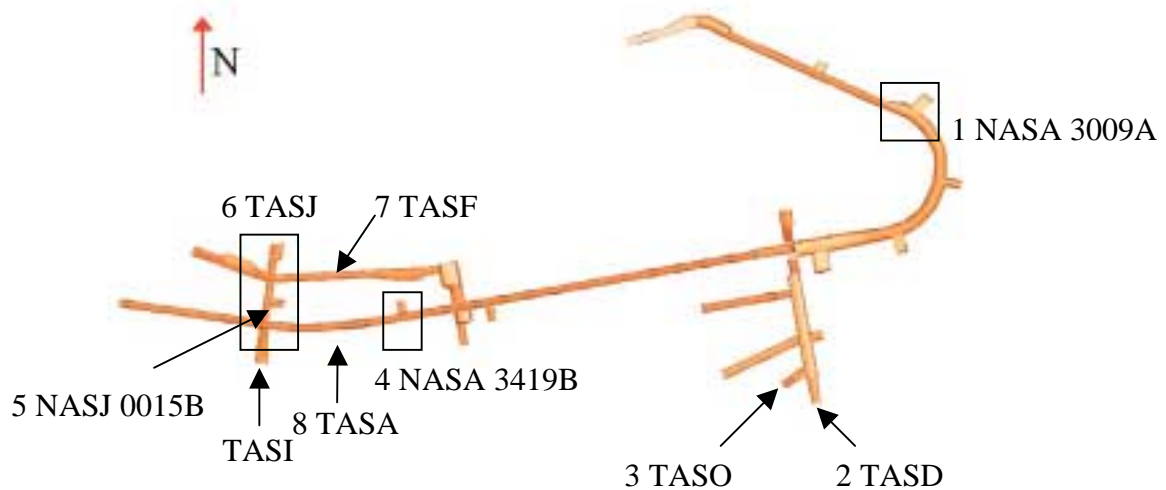


Figure 4-2. Final areas selected for numerical modelling.

4.3 Modelling results

The results from the modelling and photographs from the different locations are presented in the following sections. Comparisons between the numerical results and the photographs are made.

4.3.1 NASA 3009A

Figure 4-3 shows the location of the niche NASA 3009A in the tunnel system.

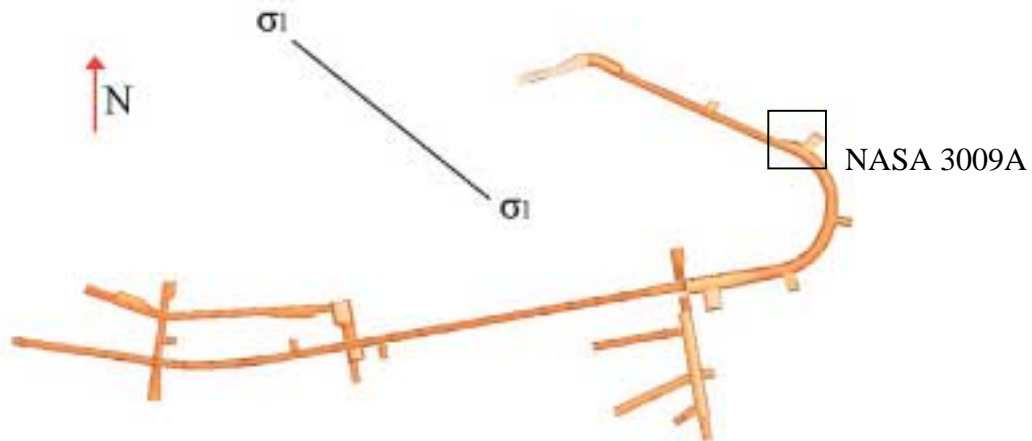


Figure 4-3. Location of NASA 3009A and a horizontal projection of the bearing of the major principal stress, σ_1 .

Scaling has been performed several times in the upper front and microseismic events were once heard during scaling. The roof and upper part of the front has been shot-creted. The isosurface for a σ_3 of 0 MPa confinement is presented in Figure 4-4.

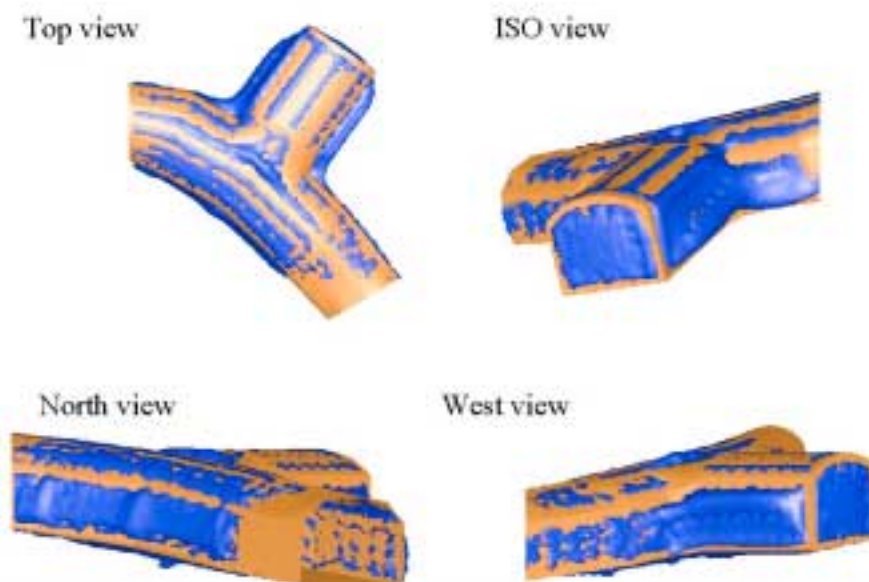


Figure 4-4. Isosurface of 0 MPa confinement at niche 3009A. North is up in the top view.

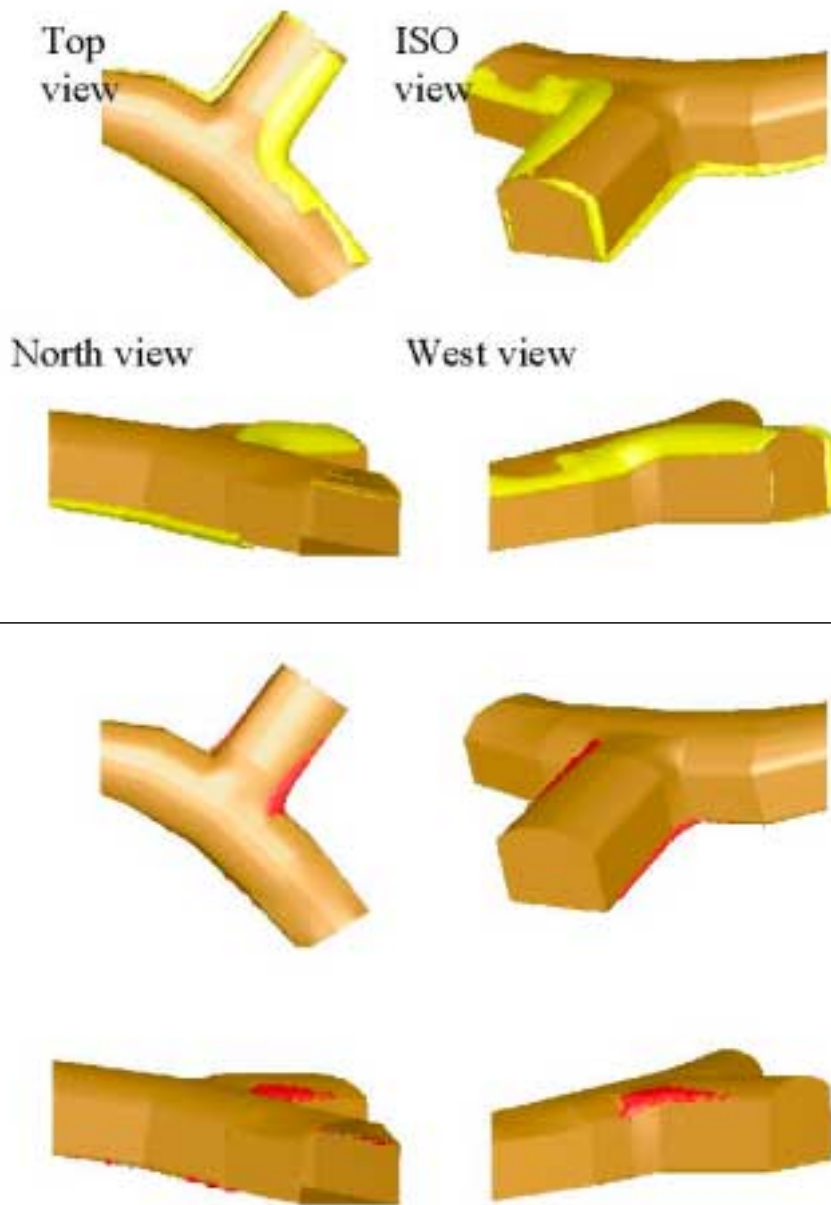


Figure 4-5. Isosurfaces for k -values of 50 MPa (yellow) and 70 MPa (red) at niche 3009A. North is up in the top view pictures.

The confinement in the niche's walls and entrance corners is low but the unconfined volume is rather small. The niche's roof and the top of the main tunnel also indicate areas of lower confinement. The isosurfaces for k -values of 50 and 70 MPa are shown in Figure 4-5.

The 50 MPa isosurface covers the west front edge of the niche and the East side of the roof. The 70 MPa surface is less pronounced which indicates that there are not that large deviatoric stresses around the niche. The low confinement in the front combined with the deviatoric stresses around the front's edge might cause the microseismic events heard. It is also probable that the scaling in the upper front depends on these factors.

Figure 4-6 shows pictures taken into the niche and down the main tunnel with the niche to the left. The need for bolts and shotcrete in the roof is probably a result of low confinement and gives some validation to the numerical results. Notice that the actual contour illustrated in Figure 4-6 is not fully implemented in the simplified numerical model. The modelling results though does not clearly indicate the microseismic events heard and the rather large scaling volumes removed.



Figure 4-6. Top photograph shows the entrance to NASA 3009A indicating the dull corners. Bottom photograph is taken down the main tunnel with the niche to the left. The blue discs are washers to the rock bolts.

4.3.2 T ASD and T ASO

Figure 4-7 shows the location of T ASD and T ASO in the tunnel system.

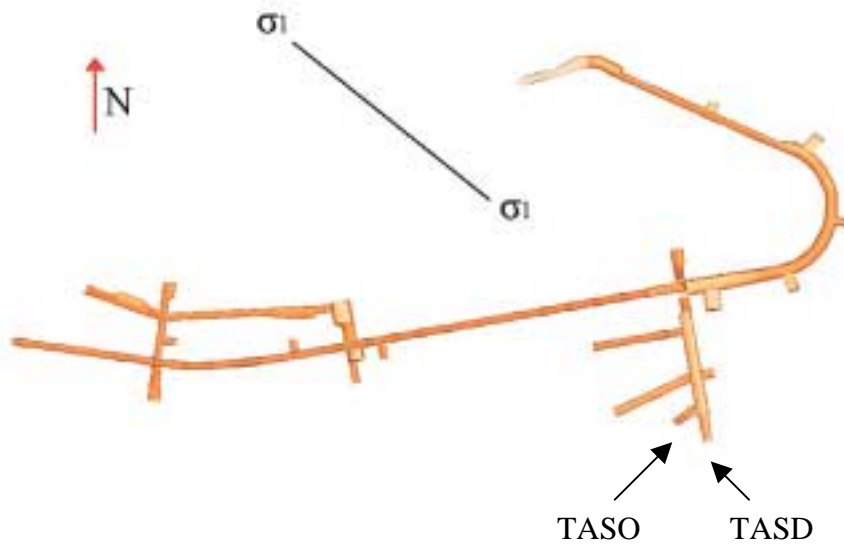


Figure 4-7. Location of T ASD and T ASO and a horizontal projection of the bearing of the major principal stress, σ_1 .

Both in the T ASD- and T ASO-tunnels microseismic events have been heard and repeated scaling carried out. Rock pieces fell from the roof in T ASO when a vibrating machine was used for compaction of backfill material in the tunnel. The isosurface for a σ_3 of 0 MPa confinement is presented in Figure 4-8.

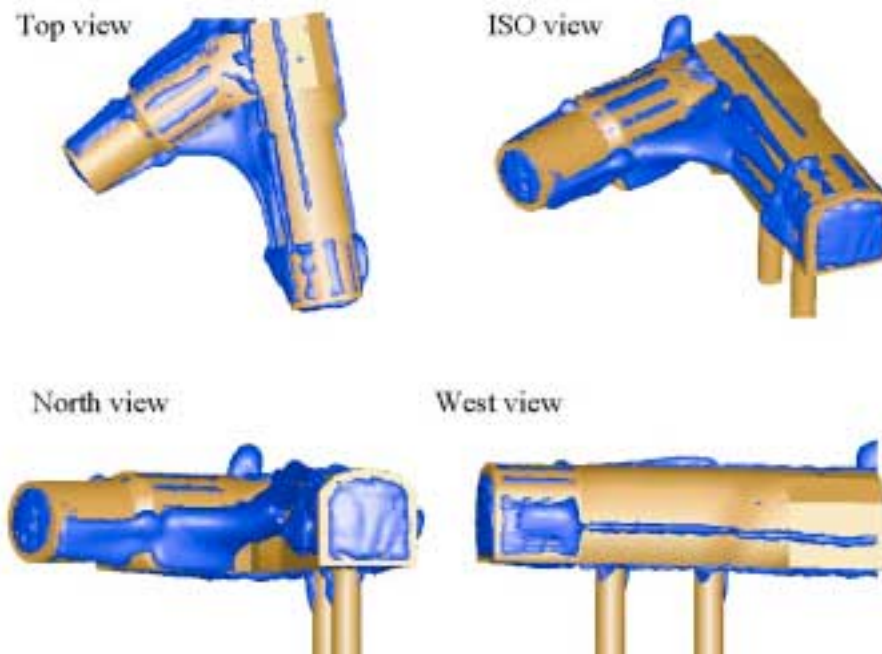


Figure 4-8. Isosurface of 0 MPa confinement at T ASO, the circular tunnel and T ASD, the horseshoe shaped tunnel. North is up in the top view.

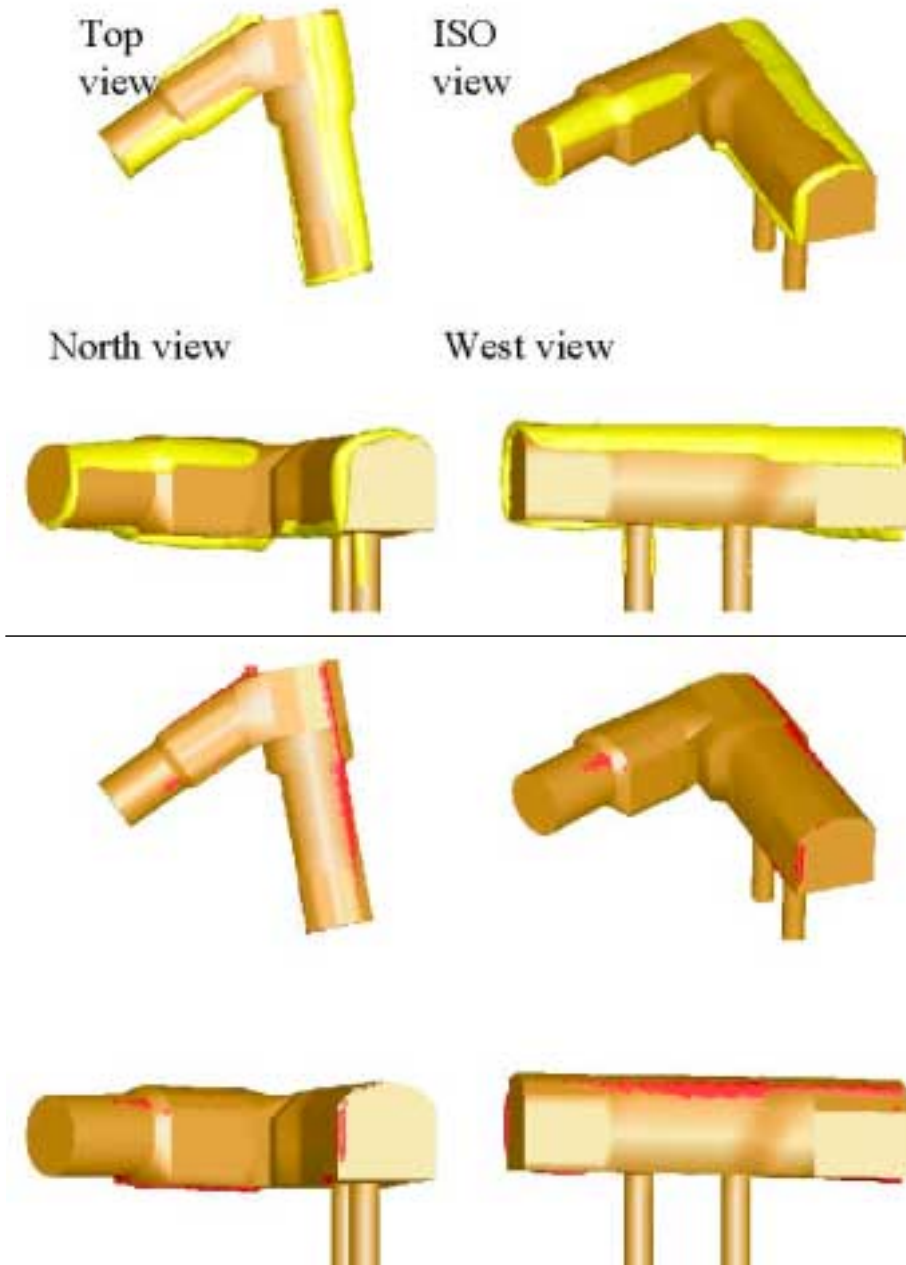


Figure 4-9. Isosurfaces for k -values of 50 MPa (yellow) and 70 MPa (red) at the O- and D-tunnels. North is up in the top view pictures.

A large part of the pillar between the two tunnels is unconfined.

The iso-surfaces for the k -values 50 and 70 MPa are shown in Figure 4-9.

The same reasoning as for niche 3009A could explain the observations made in these tunnels. To find out if the local stress situation could be affected by the close lying deformation zone NE-1 (see Figure 2-7) two additional realisations were made. The stress field was turned both 30 degrees clockwise and 30 degrees counter clockwise in relation to the general stress field used. The results were very similar to the realisation where the general stress field was used and result figures from these realisations are

therefore not presented and it is concluded that NE-1 not affects the local stress situation.

The low confinement in the pillar between the tunnels has not led to additional scaling and the corner is still pretty sharp. The reason for this is probably sparse fracturing in combination with favourable fracture orientations. Figure 4-10 shows the T ASD-tunnel to the left and the T ASO-tunnel to the right. Figure 4-11 is a photograph of the support in the front of the T ASD-tunnel. The support is highly over dimensioned since a long-term experiment is carried out in the tunnel.



Figure 4-10. Photograph of the T ASD-tunnel to the left and T ASO-tunnel to the right. Bottom picture is a close-up on the pillar between the tunnels. The pillar is rather unaffected by its low confinement and is sparsely bolted.



Figure 4-11. Photograph of the front of the D-tunnel and its support.

4.3.3 NASA 3419B

Figure 4-12 shows the location of the niche NASA 3419B in the tunnel system.

This niche was selected since additional scaling had to be done after heating of the roof due to the use of a compressor. The isosurface for a σ_3 of 0 MPa confinement is presented in Figure 4-13.

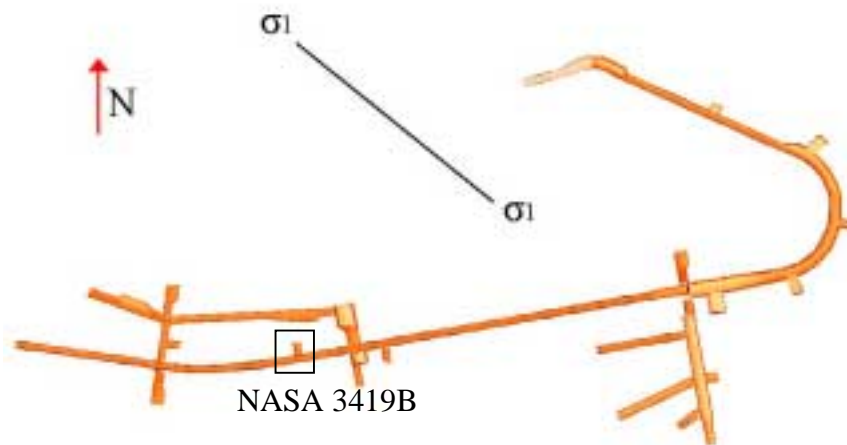


Figure 4-12. Location of NASA 3419B and a horizontal projection of the bearing of the major principal stress, σ_1 .

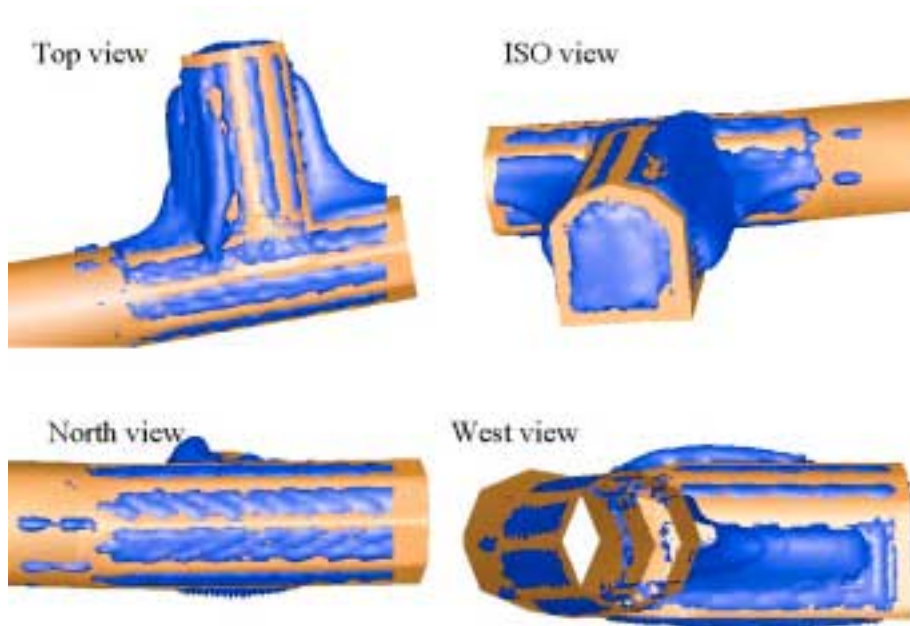


Figure 4-13. *Isosurface of 0 MPa confinement at NASA 3419B. North is up in the top view.*

The corners and the upper part of the west wall are in low confinement as well as the TBM-tunnel walls adjacent to the corners.

The isosurfaces for the k -values 50 and 70 MPa are shown in Figure 4-14.

The deviatoric stresses in the upper east half of the niche is probably close to the strength of the rock mass. The area of the 50 MPa isosurface is covering approximately half of the roof area.

Figure 4-15 shows photographs of the niche taken looking east and west. The scaling in the corners was made during excavation but supports the result indicating low confinement close to the TBM tunnel. The rather high stresses in the tunnel roof makes it probable that the heating from the compressor have accelerated the need for scaling. Approximately 2 m^3 was scaled after the compressor had been used. It is therefore likely that spalling is taking place in the right wall and loosening of rock by gravitational forces in the left wall. The scaling volumes are approximately the same in each of the walls and the roof.

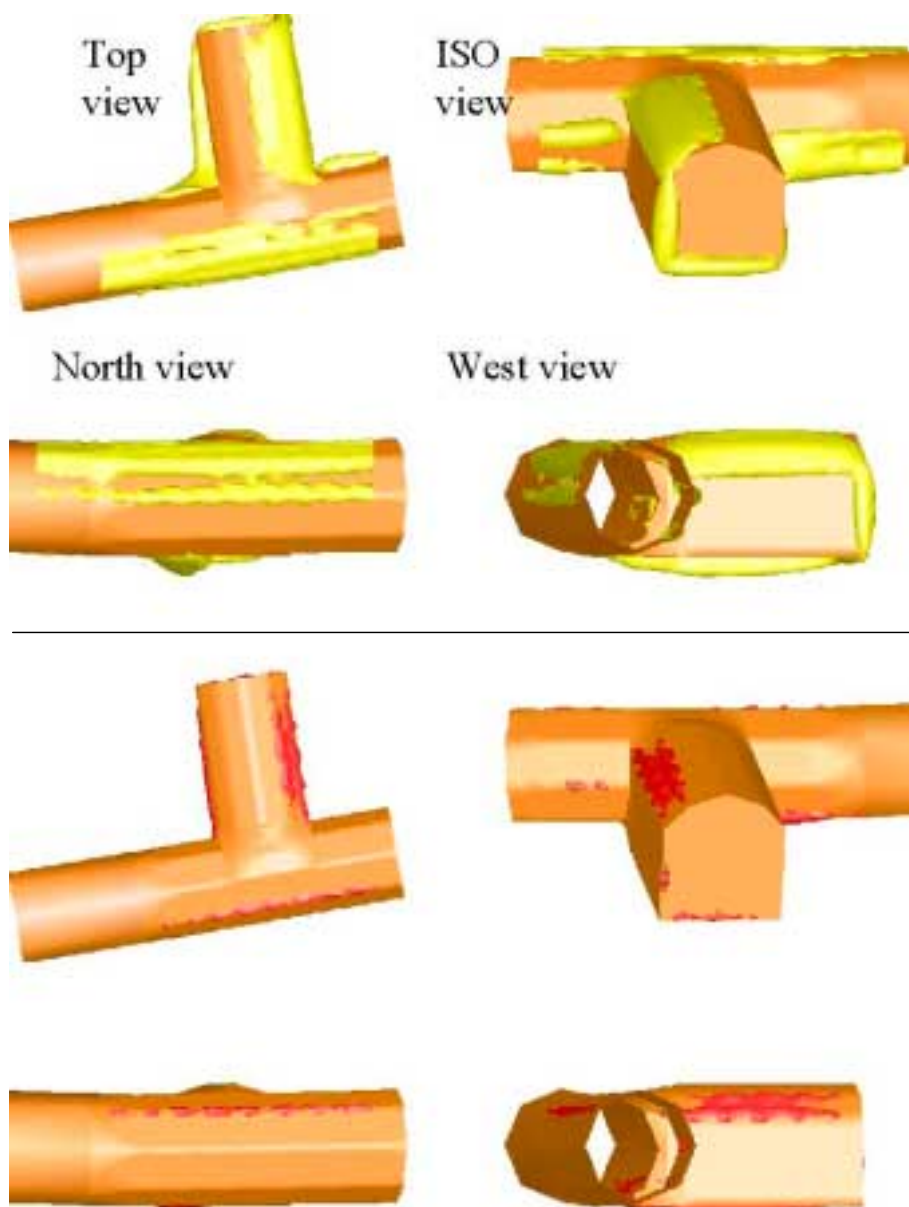


Figure 4-14. Isosurfaces for k -values of 50 MPa (yellow) and 70 MPa (red) at niche NASA 3419B. North is up in the top view pictures.



Figure 4-15. Top photograph taken looking east and bottom photograph taken looking west shows the entrance of niche 3419B. Note the intact TBM-tunnel on both sides of the niche.

4.3.4 TASJ and its crossing with TASA and TASI

Figure 4-16 shows the location of TASJ in the tunnel system.

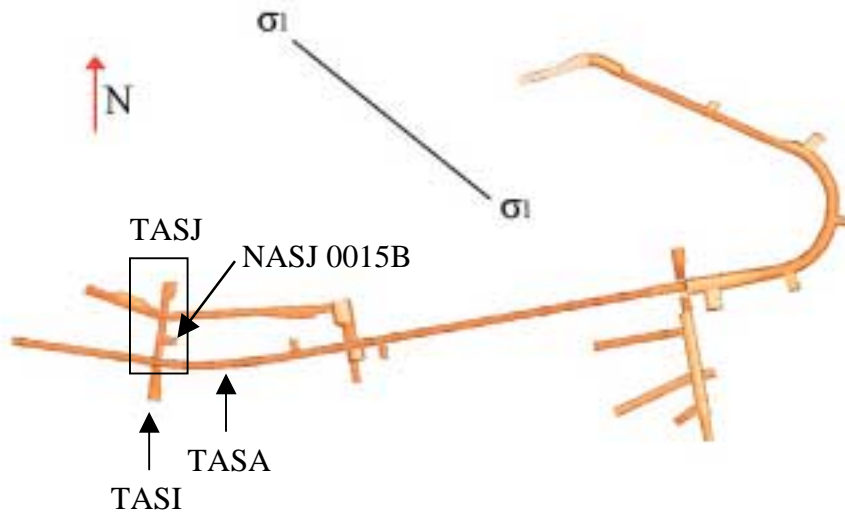


Figure 4-16. Location of TASJ, TASA, TASI and a horizontal projection of the bearing of the major principal stress, σ_1 .

This part of the tunnel system has needed repeated scaling. No larger volumes have been removed on each time separate time though. The roof was bolted, meshed and later shotcreted. The isosurface for a σ_3 of 0 MPa confinement is presented in Figure 4-17. The north view in the figures has been removed since it not gives any additional information.

The grid for this realisation is not as dense as the one used for modelling of the niche NASJ 0015B. The niche is therefore presented separately.

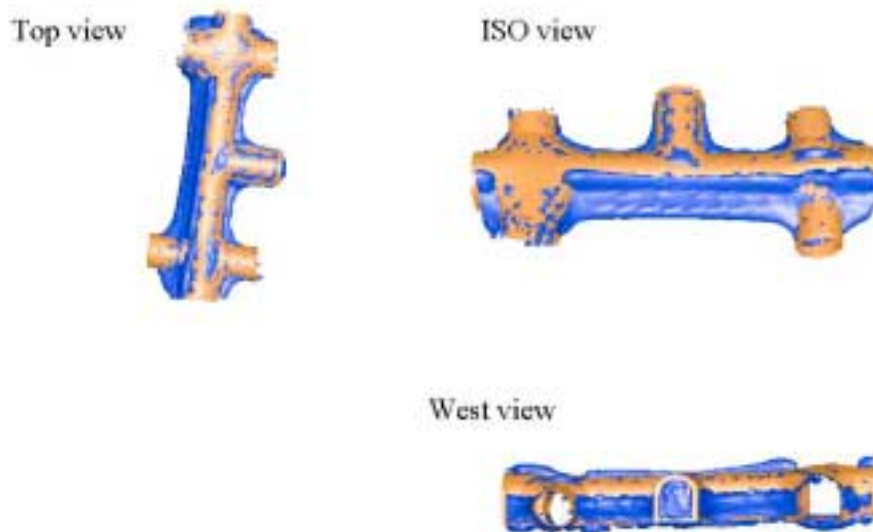


Figure 4-17. Isosurface of 0 MPa confinement at the J-tunnel. North is up in the top view.

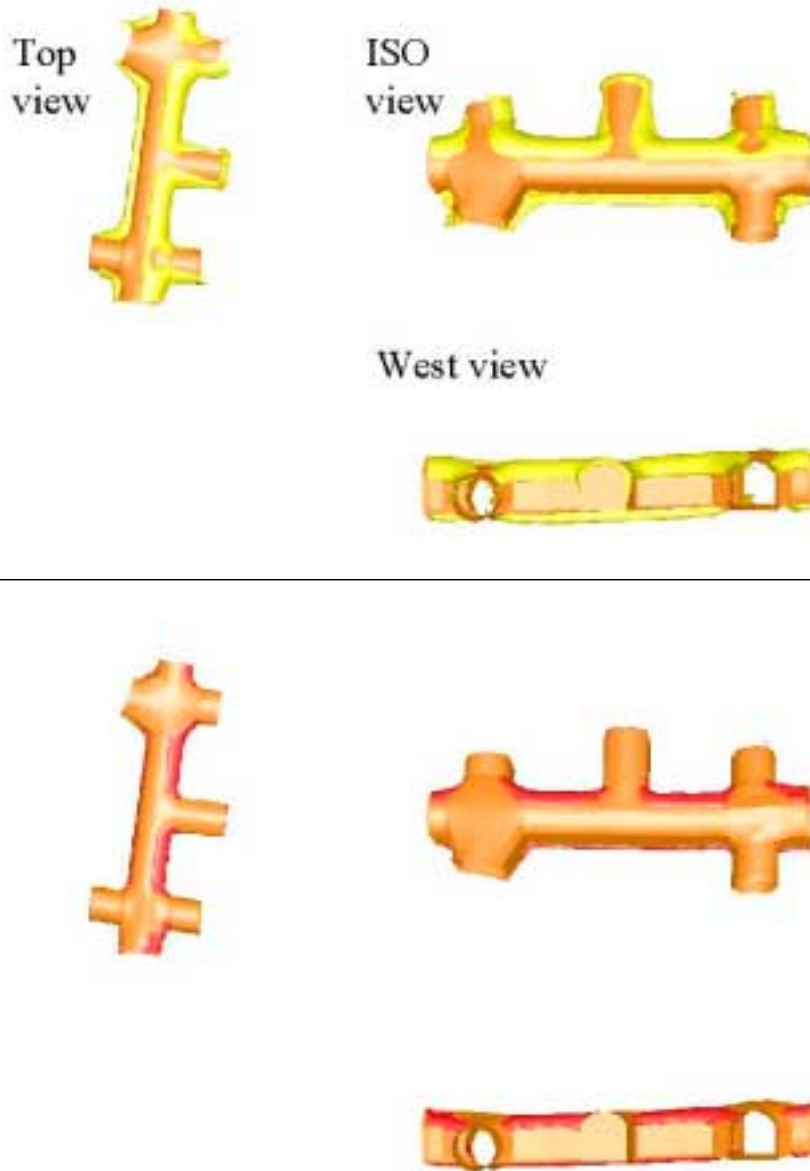


Figure 4-18. Isosurfaces for k -values of 50 MPa (yellow) and 70 MPa (red) at the J-tunnel. North is up in the top view pictures.

Both the west and east walls are without confinement one to two meters into the tunnel walls.

The isosurfaces for the k -values of 50 MPa and 70 MPa are shown in Figure 4-18.

There are large deviatoric stresses in the upper part of the east wall. The 50 MPa isosurface covers the major part of the roof. The roof is unloaded on the West side and subjected to rather large deviatoric stresses on the East side.

Figure 4-19 shows a photograph of TASJ with the niche NASJ 0015B to the right. The photograph is taken standing in the crossing between TASA, TASI and TASJ.



Figure 4-19. TASJ with NASJ 0015B to the right.

4.3.5 NASJ 0015B

Figure 4-20 shows the location of NASJ 0015B in the tunnel system.

The front of NASJ 0015B has been scaled several times. The scaling has been performed in the front of the niche. The geology of the niche consists of fractured Småland granite. The isosurface for a σ_3 of 0 MPa confinement is presented in Figure 4-21.

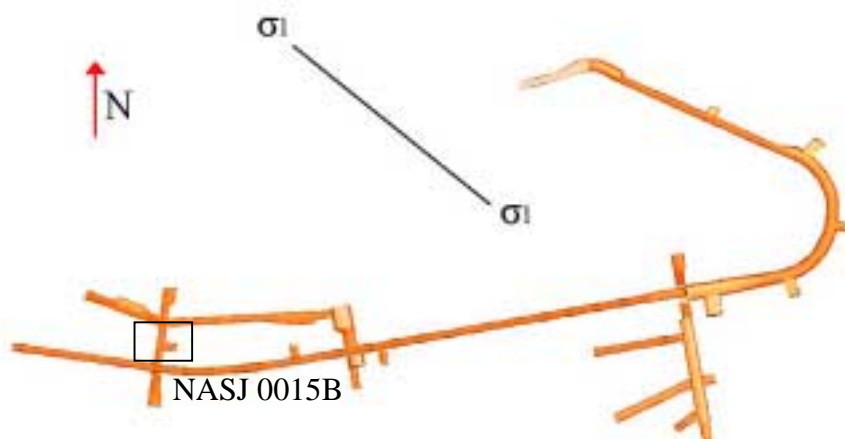


Figure 4-20. Location of NASJ 0015B and a horizontal projection of the bearing of the major principal stress, σ_1 .

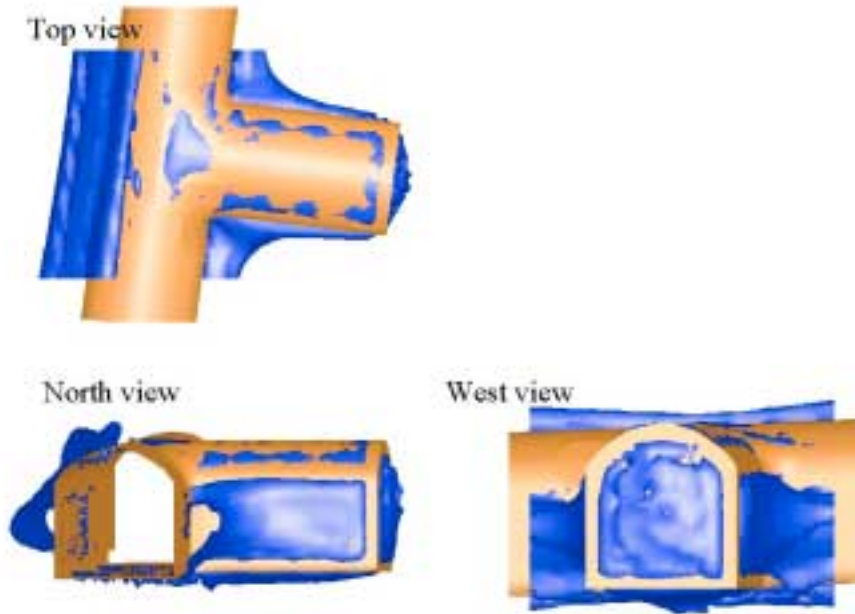


Figure 4-21. Isosurface of 0 MPa confinement at niche NASJ 0015B. North is up in the top view.

The unconfined volumes around the niche are rather limited.

The isosurfaces for the k-values of 50 MPa and 70 MPa are shown in Figure 4-22.

There are large deviatoric stresses in the upper part of the entrance on both sides as well as around the edge of the front.

Figure 4-23 shows two photographs from different parts of the tunnel front. The brittle Småland granite together with the large deviatoric stresses around the front's edge and the rather large unconfined volume in the front could very well explain the need for additional scaling. The entrance of the niche is shown in Figure 4-19.

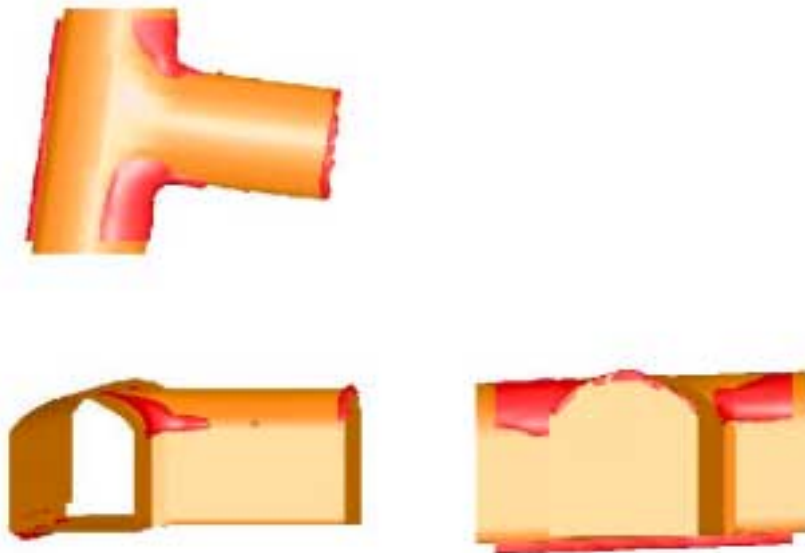
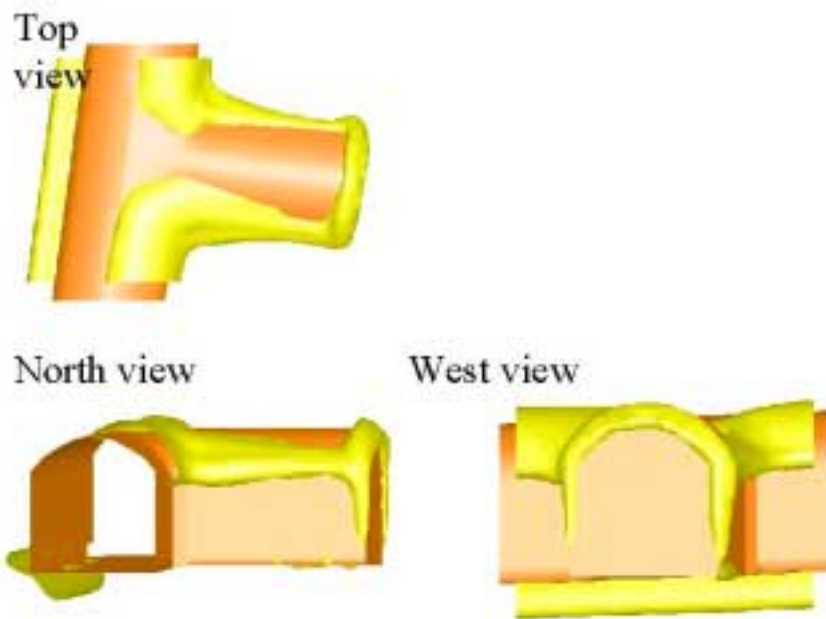


Figure 4-22. Isosurfaces for k -values of 50 MPa (yellow) and 70 MPa (red) at niche NASJ 0015B. North is up in the top view pictures.

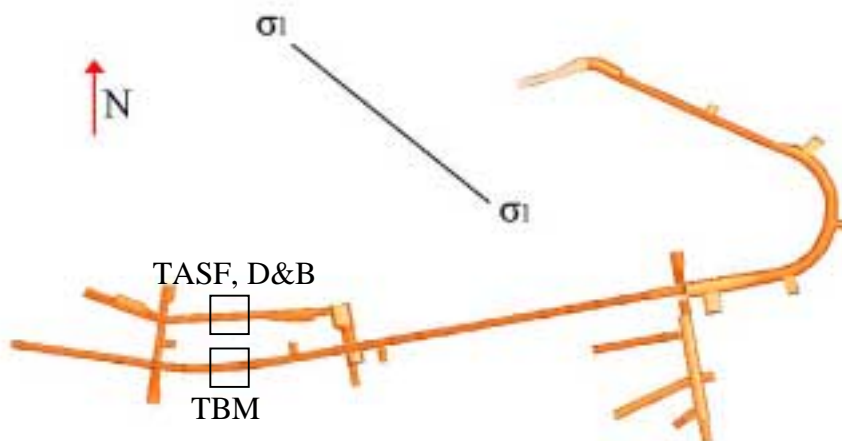


Figure 4-23. Two photographs of the front of niche NASJ 0015B.

4.3.6 Comparison TBM and D&B

Figure 4-24 shows the location of the areas of the TBM-tunnel, TASA and the D&B-tunnel (TASF) that have been modelled.

As mentioned in section 3.3 the drill and blast tunnel, TASF, have required more maintenance than the rest of the drill and blast tunnels. The interesting thing here is that the adjacent TBM tunnel hasn't required any maintenance at all. Two parallel parts of the TBM- and TASF-tunnel have therefore been numerically modelled to see the differences in the stress situation around them. The modelled areas have been selected in such a way that they are not influenced by disturbances in the in situ stress field caused by the other tunnels and niches.



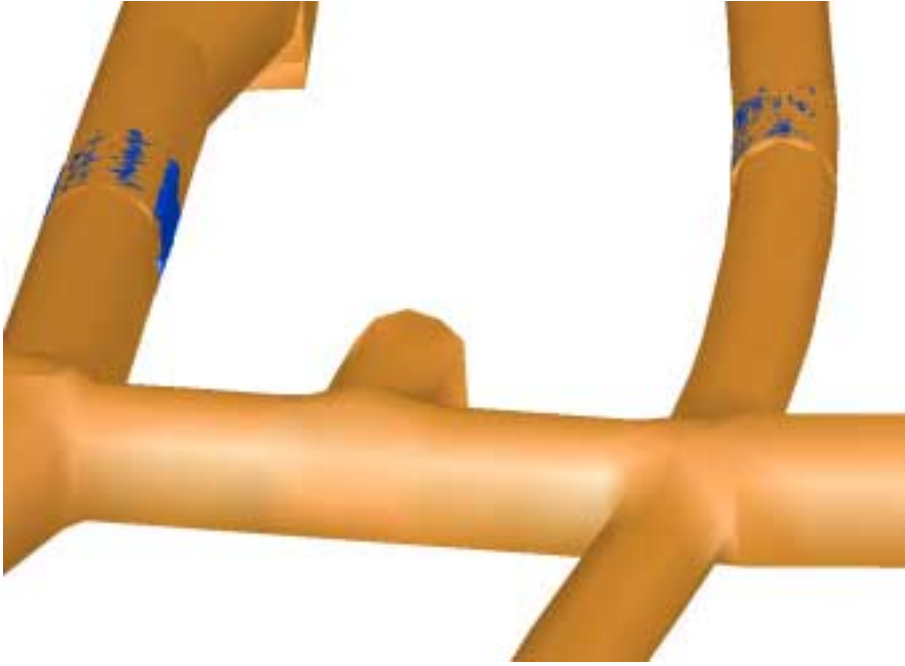


Figure 4-25. *Isosurfaces of 0 MPa at TASF, left and the TBM-tunnel, right. NASJ 0015B is the niche between the tunnels.*

Figure 4-25 to Figure 4-27 shows the results from the numerical modelling.

As indicated by Figure 4-25 to Figure 4-27 the volume of rock with low confinement is much larger in the D&B tunnel than in the TBM tunnel. The deviatoric stresses close to the two tunnels are quite low. The 60 MPa isosurface is hardly visible if plotted. Figure 4-28 is a photograph of the TASF-tunnel.

The probable reason for the maintenance need in the D&B-tunnel is the combination of low confinement, fractured granites and gravitational forces.



Figure 4-26. *Isosurfaces of the minor principal compressive stress at magnitudes of 0 MPa (dark blue), 3 MPa (light blue) and 6 MPa (green). TASF to the left and the TBM-tunnel to the right.*

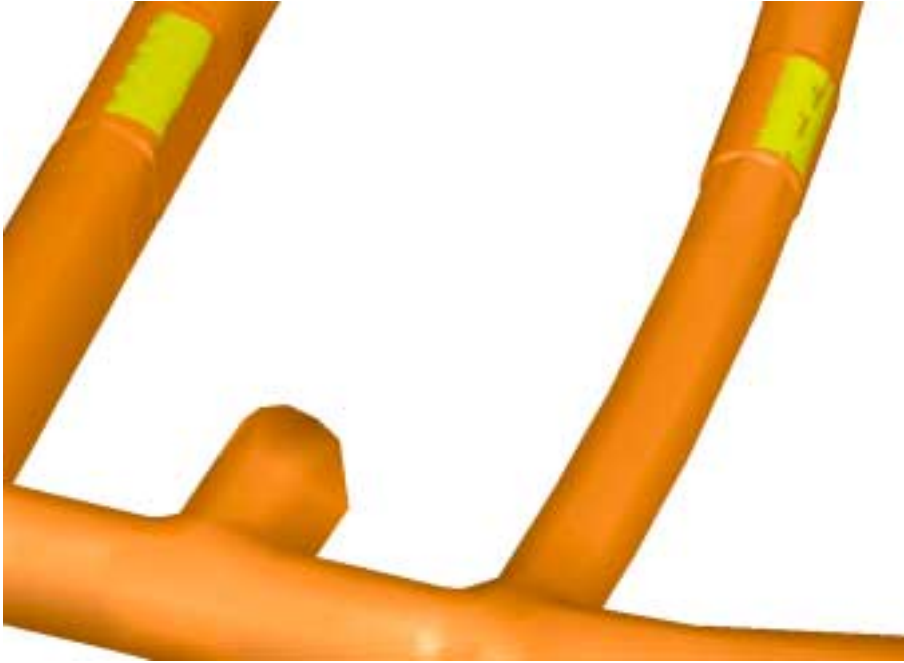


Figure 4-27. Isosurfaces for a k-value of 50 MPa. TASF to the left and the TBM-tunnel to the right.



Figure 4-28. Top photograph is taken down the TASF-tunnel.

5 Discussion

The results from the compilation of maintenance data presented in section 3 and the results from the numerical modelling in section 4 are here further discussed.

5.1 Maintenance

One has to give emphasis to the fact that the major part of Äspö HRL is a stable facility from a rock mechanics point of view. The additional maintenance described in this report is only carried out in a very limited part of the tunnel system. It is still possible to see traces of most of the drill-holes for the blasting in the contour. This is a good indication that the facility is stable without stress corrosion going on in the analytically studied parts.

When looking at the results in Figure 3-3 the first eye catchers are leg# 3 and 4. No maintenance activities have had to be performed here during the operational phase of Äspö HRL. The normalised scaling volumes are slightly lower than average for the studied part of the tunnel. These legs also include the two parts of the tunnel with the lowest RMR-values. The RMR-values are never lower than 40 in the tunnels and the rock mass is therefore classified as “fair rock”. The water inflow according to Figure 3-4 is slightly lower than the average inflow. The two leg’s relation to the major principal stress is quite opposite. Leg 3 is almost parallel to it and leg 4 deviate approximately 60 degrees from the bearing of the major principal stress. The most obvious difference between these legs and the others is that they are located furthest away from any of the deformation zones located in the vicinity of Äspö HRL.

After studying the maintenance records it is clear that almost all of the bolting have been performed in the curves where the tunnel is widened. One reason could be that the rock is more fractured from the blasting when widening the tunnel. The records though indicates that increased scaling only have had to be performed in two of the curves. The additional bolting in the other curves could therefore partly have been done of psychological reasons because of the wider tunnel and perhaps more fractured surface than the actual need for maintenance. The tunnel contour in the outside of the curves is rougher than the contour in the straight part of the ramp due to the D&B and might therefore look a bit more unstable.

It is clear that all bolting, shotcreting and scaling is located to either Äspö diorite areas with intrusions of Fine-grained granite or larger areas with Småland granite. Increased fracturing or fracture zones often occur in the Fine-grained granite and Småland granite. This is probably the reason for the need for maintenance in these parts.

Maintenance has been conducted in the straight middle part (the area between the curves) of three of the legs. When the angle between a tunnel and the major principal stress increases the deviatoric stresses in the tunnel roof also increases and the tunnel walls get subjected to tensile stresses. Areas with this kind of stresses are likely to need more maintenance than tunnel legs parallel to the major principal stress. Five of the

legs, No. 1, 2, 4, 5 and 7 are maintained in their straight middle part and diverting about 60 degrees from the major principal stress. Leg# 8 is not supported but evenly scaled along its straight part and the normalised scaling for this leg is the highest for the studied legs.

If the bolting in the fracture zone area in leg# 9 is excluded there is almost no maintenance in the tunnel legs almost parallel to the bearing of the major principal stress.

5.2 Water inflow

It is well recognised at Äspö HRL that the most water bearing structures are striking NNW-ESE, hence in the bearing of the major principal stress. The tunnel legs with a large angle to the principal stress bearing therefore intersect more water bearing features and hence should have a higher water inflow. Three of the legs with a large angle to the major principal stress show this behaviour. The other three have approximately the same normalised inflow as the legs parallel to the major stress bearing. Leg# 9 that is almost parallel to the major stress bearing has the highest water inflow of them all.

The comparison of the three different facilities Äspö HRL, SFR and CLAB clearly shows that a rather constant decrease of the water flow in the facilities is taking place. The decrease in the facilities is remarkable uniform and is approximately 4% per year. Since SFR is located in another part of Sweden than Äspö HRL and CLAB the decrease can not be regarded as a local phenomena. It is also interesting that the decrease is so uniform since Äspö HRL is much less grouted than the other facilities.

5.3 Numerical modelling

In general the results from the numerical modelling agrees reasonably well with the observations made in the tunnels. The following paragraphs will comment the results from the numerical modelled areas of the tunnel.

The behaviour of niche NASA 3009A (section 4.3.1) corresponds rather well to the results obtained by the numerical modelling. The unloaded centre part of the front and deviatoric stresses in the front's corner and roof could explain the need for additional scaling.

The modelling of the T ASD- and T ASO-tunnels (section 4.3.2) also corresponds well to the actual behaviour of the tunnels. The deviatoric stress in the west corner of T ASD is recognised in the tunnel since this part is much drummier than the east corner. From the photograph in Figure 4-10 it can be seen that more shotcrete is placed on the east wall than on the west. The numerical results indicate lower confinement in the upper part of the west wall and deviatoric stresses on the upper part of the east wall. In the front of T ASO there is a vein of pegmatite and granite close to the south corner. The micro-seismic events heard in the tunnel could very well come from that more coarse grained and probably weaker rock type when stresses were redistributed during the scaling.

The response of niche NASA 3419B (section 4.3.3) to the heating from the compressor is a good indicator that the rock mass behaviour is approaching a brittle instead of elastic response in this stress field. The numerical modelling indicates rather large deviatoric stresses in the roof. The induced stress due to the thermal expansion was probably enough to create minor spalling and relatively large volumes of small rock blocks where scaled. Some scaling has also been done in the TBM-tunnel wall adjacent to the niche, which according to the numerical modelling is unloaded.

The numerical results for the TASJ-tunnel (section 4.3.4) indicates large deviatoric stresses in the upper east part of the wall and roof and low confinement of the whole west wall and the lower part of the east wall. The magnitude of the deviatoric stresses makes it probable that stress corrosion have taken place and hence the need for scaling and later shotcreting.

The unloaded volume in the front of niche NASJ 0015B (section 4.3.5) is rather large. Most of the scaling in this niche has been performed here. There are also higher deviatoric stresses in the upper part of the front and the upper part of the entrance corners. When looking at Figure 4-19 one can see that the area with large deviatoric stresses in the upper entrance corners has been scaled.

Several lab rock strength measurements have been performed before and during the operational phase of the laboratory. Results from triaxial and unconfined compressive strength measurements as well as results from Brazil tests are compiled in Figure 5-1. The figure includes a best-fit second-order polynome line and a crosshatched area indicating the probable spread of the rock strength. Some maximum stresses resulting from the numerical calculations in NASA 3419B and the TASJ-tunnel are also included. The results have been taken from the 20 cm of rock closest to the tunnel wall/roof in the most stressed parts of the two areas. The modelled stresses are clearly lower than the

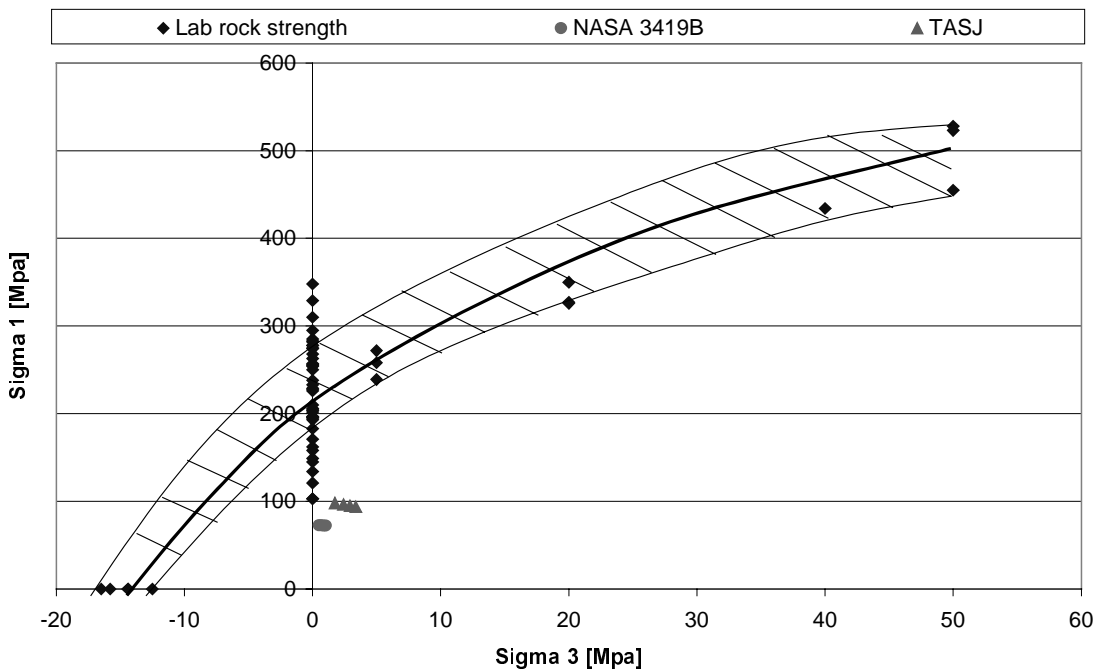


Figure 5-1. Compilation of lab rock strength measurements and results from highly stressed areas according to the numerical modelling.

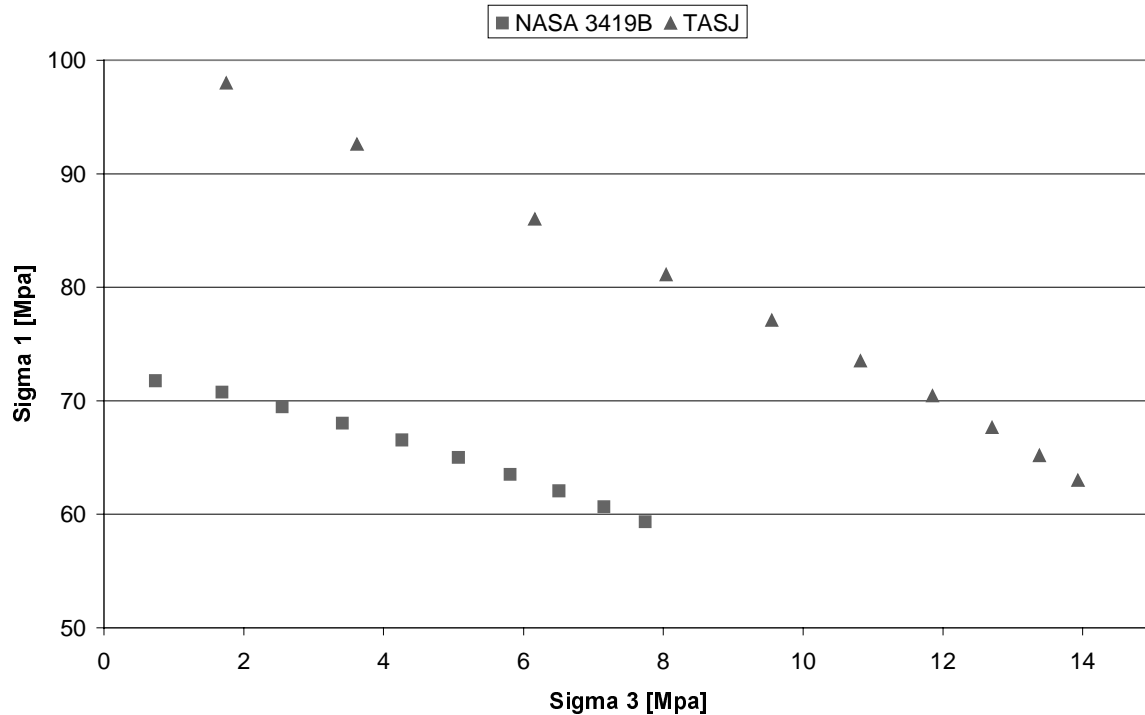


Figure 5-2. The stress situation in the 50 cm of rock closest to the tunnel contours in NASA 3419B and TASJ.

failure envelop. However, during Young’s modulus measurements it is indicated that microcracks are induced when the biaxial applied stress reaches approximately 100 Mpa.

The results from the numerical modelling presented in Figure 5-1 are shown in Figure 5-2 in an enlarged graph. The markers in the graph are evenly distributed in the closest 50 cm of the rock from the tunnel contour in the highest stressed areas.

The stress situation in especially TASJ is very close to the one where crack initiation could be expected. This is also indicated by the fact that this area is the most maintained of the ones studied. It is assessed that the stress situation in NASA 3419B could reach the same levels as at TASJ when heated approximately 50 degrees C. This would in that case explain the need for scaling when the compressor was removed.

Martin et al. /1999/ presents a relationship between the depth of failure and the maximum tangential stress at the boundary of an opening. The linear relationship was presented as equation (5-1):

$$\frac{Rf}{a} = 0.49(\pm 0.1) + 1.25 \frac{\sigma_{\max}}{\sigma_c} \quad (5-1)$$

where the depth of failure (Rf) is normalised to the effective tunnel radius (a) and that the failure initiates when $\sigma_{\max}/\sigma_c \approx 0.4 \pm 0.1$. The maximum stress obtained from numerical modelling is approximately 100 MPa and the unconfined compressive

strength for Äspö diorite is approx. 200 MPa. Using these values the σ_{\max}/σ_c ratio is 0.5. According to Martin et al. this is very close to the limit to where spalling is initiated.

When comparing the D&B and the TBM-tunnel one would expect larger differences in the local stress fields around the tunnels since the maintenance situations are totally opposite. The TBM-tunnel is totally intact while the D&B-tunnel have required a lot of scaling and bolting during the operational phase until it was decided to shotcrete the roof and the upper parts of the walls. The numerical results indicated that there is a much larger zone with low confinement in the walls of the D&B-tunnel. The deviatoric-stressed zones are similar in the two cases and do not indicate that the D&B-tunnel should be more unstable than the TBM-tunnel. The deviatoric stresses in both cases should not be able to cause failure in the rock mass. The difference in maintenance need is therefore probably caused by the Småland granite and the fine-grained granite, which often are more fractured than the Äspö diorite.

6 Conclusions

The study of the maintenance records indicates that the reason for the additional maintenance in different parts of the main tunnel (TASA) is due to geological factors. The scaling, bolting and shotcreting are located in areas with intrusions or veins of Fine-grained granite or Småland granite. Increased fracturing and fracture zones are typically associated to these two rock types. It can therefore be concluded that no stress corrosion is going on in the main tunnel. The situation in the niches and side-tunnels studied is though a bit different. The location and orientation of the studied objects have been made without rock mechanics considerations. The support and scaling performed there is most certainly caused by stress concentrations created by the choice of geometry. The stress concentrations seem to be of minor importance with the stress field used in the models at 420 m depth. When the stress magnitudes are increased for the modelling of the 450 m level the induced stresses are close to the strength of the rock mass. Good examples of this are the TASJ-tunnel and niche NASA 3419B. The numerical modelling indicates large deviatoric stresses where support and scaling has had to be done. The behaviour of the rock mass indicates that it is leaving its elastic response stage and approaching a more brittle behaviour. One example of this is the need for scaling in NASA 3419B after its roof was heated with the exhausts from a diesel compressor. The rock mass behaviour corresponds well to the measured rock strength and its behaviour observed during biaxial testing. In the most stressed parts of the different models the rock mass is very close to spalling. Stress corrosion might therefore very well occur in limited parts of these areas since the actual geometry could be less favourable than the one used for modelling.

There is an indication that the tunnel alignment to the stress field has an impact on the need for maintenance.

The numerical stress modelling performed agrees rather well with the observations made in the modelled areas. Areas in the models indicating high stresses or low confinement could in most cases be correlated to actual observations. The results are not so clear though that all the problems easily could have been foreseen without the interview and the maintenance records, at least at the 420 m level.

The comparison of a horseshoe shaped D&B-tunnel with a TBM-tunnel regarding the need for maintenance clearly shows that the drill and blast tunnel requires much more resources in that aspect. The maintenance free TBM-tunnel is a clear contrast to the repeatedly scaled, bolted and finally shotcreted D&B-tunnel. The numerical modelling do not give a clear indication that this should be the case. The maximum deviatoric stresses are approximately the same but the volume of low confinement in the tunnel's walls is much larger for the D&B-tunnel. Since the Småland granite and the fine-grained granite often are more fractured than the Äspö diorite it is likely that these areas in TASF also is rather fractured and needs additional scaling.

It is likely that the stability of the tunnel system would decrease if the tunnels were located at 500 m depth. The geometry is therefore of most importance when designing a facility at these depths in this kind of rock. If the tunnel system was subjected to the in situ stresses at approx. 550 m depth it is assessed that the rock mass response would be

brittle instead of elastic. A future repository for spent nuclear fuel will be located at a depth somewhere between 400 to 700 m. Hence, the design of the transport and service tunnels as well as the underground caverns for different activities has to be designed very carefully. They will be intensively used for 50 to 100 years and repeated maintenance needs due to bad design will be both costly and probably disturb the operations in the facility.

References

Ask D, Stephansson O, Cornet F, 2001. Äspö Hard Rock Laboratory. Integrated stress analysis of hydraulic stress data in the Äspö region, Sweden. Analysis of hydraulic fracturing stress measurements and hydraulic test in pre-existing fractures (HTPF) in boreholes KAS02, KAS03 and KLX02. SKB IPR-01-26, Svensk Kärnbränslehantering AB.

Hakami E, Hakami H, Cosgrove J, 2002. Strategy for a descriptive rock mechanics model. Development and testing of an Approach to MODELING the state of stress. SKB R-02-03, Svensk Kärnbränslehantering AB.

Hedman T, 1999. Äspö Hard Rock Laboratory. Experience from design and construction. SKB IPR-99-05, Svensk Kärnbränslehantering AB.

Hudson J A (Editor), 2002. Strategy for a descriptive rock mechanics model. A test case based on data from the Äspö HRL. SKB R-02-04, Svensk Kärnbränslehantering AB.

Makurat A, Löset F, Wold Hagen A, Kveldsvik V, Grimstad E, 2002. Äspö HRL. A descriptive rock mechanics model for the 380–500 m level. SKB R-02-11, Svensk Kärnbränslehantering AB.

Markström I, Erlström M, 1996. Äspö Hard Rock Laboratory. Overview of documentation of tunnels niches and core boreholes. SKB Äspö Progress Report HRL-96-19, Svensk Kärnbränslehantering AB.

Martin C D, Kaiser P K, McCreath D R, 1999. Hoek-Brown parameters for predicting the depth of brittle failure around tunnels. Canadian Geotechnical Journal 36(1):136–151.

Martin C D, Christiansson R, Söderhäll J, 2001. Rock stability considerations for siting and constructing a KBS-3 repository. based on experiences from Äspö HRL, AECL's URL, tunneling and mining. SKB TR-01-38, Svensk Kärnbränslehantering AB.

Nilsson R, 2000. Södermans Bergsprängning AB. Personal communication 2000-11-07.

Nordlund E, Chunlin L, Carlsson B, 1999. Äspö HRL Prototype Repository, Mechanical properties of the diorite in the prototype repository at Äspö HRL. SKB IPR-99-25, Svensk Kärnbränslehantering AB.

Rhén I, Gustafson G, Stanfors R, Wikberg P, 1997. Äspö HRL – Geoscientific evaluation 1997/5. Models based on site characterisation 1986–1995. SKB TR 97-06, Svensk Kärnbränslehantering AB.

Rummel F, Klee G, Weber U, 2002. Rock stress measurements in Oskarshamn. Hydraulic fracturing and core testing in borehole KOV01. SKB IPR-02-01, Svensk Kärnbränslehantering AB.

Röshoff K, Lanaro F, Jing L, 2002. Strategy for a descriptive rock mechanics model. Development and testing of the Empirical approach. SKB R-02-01, Svensk Kärnbränslehantering AB.

Staub I, Fredriksson A, Outters N, 2002. Strategy for a descriptive rock mechanics model. Development and testing of the Theoretical approach. SKB R-02-02, Svensk Kärnbränslehantering AB.